

**Effects of Graphene Coating on $\text{Li}_2\text{Fe}_{0.5}\text{Mn}_{0.5}\text{SiO}_4$ Cathode Materials
for Thin-Film Lithium-Ion Batteries**

A Major Qualifying Project Report

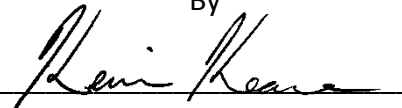
Submitted to the Faculty and Staff of

WORCESTER POLYTECHNIC INSTITUTE

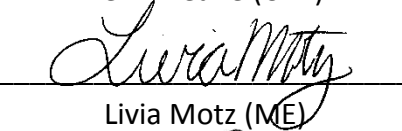
In partial fulfillment of the requirements for the

Degree of Bachelor of Science

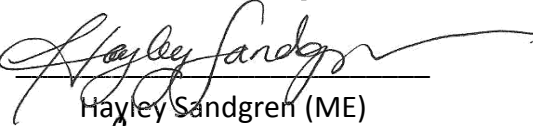
By



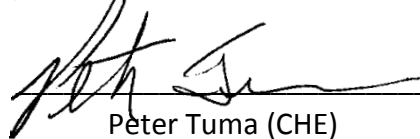
Kevin Keane (CHE)



Livia Motz (ME)



Hayley Sandgren (ME)

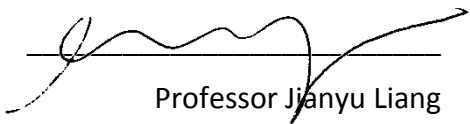


Peter Tuma (CHE)

Approvals:

Professor David DiBiasio

Chemical Engineering Advisor



Professor Jianyu Liang
Mechanical Engineering Advisor

Abstract

In this project, we studied the effect that carbon coating with graphene has on the performance of $\text{Li}_2\text{Fe}_{0.5}\text{Mn}_{0.5}\text{SiO}_4$ cathode materials for lithium-ion batteries. We synthesized the $\text{Li}_2\text{Fe}_{0.5}\text{Mn}_{0.5}\text{SiO}_4$ cathode materials, tested the performance with coin-cell battery testing, and characterized the composites through SEM and XRD analysis. Results are promising, indicating improved discharge capacity of the batteries and exceptional current efficiency, making graphene-coated $\text{Li}_2\text{Fe}_{0.5}\text{Mn}_{0.5}\text{SiO}_4$ cathode materials a significant advance in energy storage.

Acknowledgements

Our group would like to extend our gratitude to Professors Jianyu Liang and David DiBiasio for the help and guidance throughout the completion of this project. We would also like to give our most sincere thanks to Yinjie Cen for the amount of time and effort put forth towards helping us complete this project.

Table of Contents

Abstract.....	ii
Acknowledgements.....	iii
Executive Summary.....	viii
1 Introduction.....	1
2 Literature Review	4
2.1 Li-Ion Batteries Background	4
2.2 Future of Lithium-Ion Batteries.....	6
2.3 Lithium-Ion Battery Mechanism	7
2.4 Lithium Silicate Materials.....	11
2.4.1 $\text{Li}_2\text{FeSiO}_4$ Polymorphs.....	12
2.4.2 $\text{Li}_2\text{MnSiO}_4$	15
2.5 2012 MQP: Synthesis, Characterization and Electrochemical Performance of $\text{Li}_2\text{Fe}_x\text{Mn}_{1-x}\text{SiO}_4/\text{C}$ as Cathode Material for Thin-Film Lithium-Ion Batteries.....	17
2.6 Graphene.....	18
2.7 Characterization	19
2.7.1 Scanning Electron Microscopy	19
2.7.2 Energy Dispersive X-ray Spectroscopy Analysis (EDX)	21
2.7.3 X-ray Powder Diffraction (XRD)	22
2.8 Electrochemical Testing	23
2.9 Summary	24
3 Methodology	25
3.1 Synthesis of Cathode Precursor	25
3.2 Synthesis of Active Cathode.....	27

3.3	Synthesis of Graphene	28
3.4	Slurry Coating Process.....	30
3.5	Coin Cell Assembly and Electrochemical Testing.....	31
4	Results and Discussion.....	33
4.1	Cathode Synthesis	33
4.1.1	SEM Analysis	33
4.1.2	XRD Analysis.....	35
4.2	Electrochemical Testing	37
4.3	Results Discussion	39
5	Conclusions and Recommendations	40
6	Appendices	41
6.1	Comparative XRD Data Findings.....	41
6.2	EDX Data.....	43
6.3	Comparative Electrochemical Test Data	44

Table of Figures

Figure 2-1: Li-Ion Battery Discharge Characteristics.....	5
Figure 2-2: A table comparing the most promising batteries of today's market.	8
Figure 2-3: Schematic cross-section of a thin-film lithium battery.	9
Figure 2-4: Layered structure of lithium cobalt oxide.	11
Figure 2-5: Spinel structure of lithium manganese oxide.....	11
Figure 2-6: Polymorphs in the space groups (a) $Pmn2_1$, (b) $P2_1/n$, and (c) $Pmnb$	14
Figure 2-7: Performance of various polymorphs.....	15
Figure 2-8: Data comparing the lithium phosphate and lithium silicate performances.	16
Figure 2-9: Destructive interface (left) and constructive interface (right) of XRD signals.	23
Figure 3-1: Flowchart of steps involved in the complete project process.	25
Figure 3-2: Mixing of solution to form gel under nitrogen flux using stirring rod.	27
Figure 3-3: Calcination of cathode precursor material.....	28
Figure 3-4: A three-neck flask with graphene oxide solution.....	29
Figure 3-5: Graphene deposits in filter.....	30
Figure 3-6: Aluminum foil coated with active cathode material.....	31
Figure 3-7: Diagram of coin-cell composition.....	32
Figure 4-1: An SEM image for pure $Li_2Fe_{0.5}Mn_{0.5}SiO_4$ baked at $700^\circ C$ for 10 hours.	34
Figure 4-2: An SEM image for pure $Li_2Fe_{0.5}Mn_{0.5}SiO_4$ baked at $700^\circ C$ for 14 hours.	34
Figure 4-3: An SEM image of graphene nanosheet.	35
Figure 4-4: XRD data showing a pure iron peak.	36
Figure 4-5: EDX images for pure $Li_2Fe_{0.5}Mn_{0.5}SiO_4$ – $700^\circ C$ for 10 hours.....	37
Figure 4-6: Comparative test data between discharge capacities of coated and uncoated silicates.....	38
Figure 4-7: Comparative test data between current efficiencies of coated and uncoated silicates.....	38
Figure 6-1: The full range of 2θ for the pure iron comparison.	41
Figure 6-2: Full comparison to lithium cobalt silicate data.	41
Figure 6-3: Full comparison to lithium cobalt silicate data.	42

Figure 0-4: 2theta comparison to previous XRD data of carbon-coated cathode material without singular, large peak.38

Figure 6-5: Comparisons of coatings on the discharge capacities from different research projects.44

Figure 0-6: Comparisons of coatings on the current efficiencies from different research projects.45

Executive Summary

As electronics and portable technologies advance, there is a growing need for batteries with increased capacity and larger energy density. Lithium-ion batteries offer a possible solution to this problem. Lithium-ion battery technology offers the advantages of high voltage and energy density, low self-discharge rate, and extremely good cycling capability. Thin-film lithium-ion batteries have been researched, but few successful prototypes have been developed. Successful prototypes have incorporated active materials such as LiCoO_2 , LiMn_2O_4 , and Li_2MSiO_4 (where $\text{M}=\text{Mn}$, Fe , Co , and Ni). Each of these materials has varying properties, including theoretical capacity, discharge voltage, conductivity, and cycling life.

Lithium silicates (Li_2MSiO_4) are candidates for future batteries due to the higher theoretical capacity, because each contains two lithium atoms in every molecule. Pure phase compounds with a general formula of Li_2MSiO_4 (where $\text{M}=\text{Mn}$ or Fe) have been tested, and results show that each presents unique advantages and drawbacks. It was found that Li_2MSiO_4 cathode materials with mixed M offer superior performance to the pure phases, much like what was observed in the case of layered LiMO_2 cathodes. Because silicate materials are not very conductive, the cathode material must be coated with a more conductive material. This can be done using carbon. In previous work, sucrose was dehydrated to obtain the carbon for the cathode coating. However, the use of sucrose did not greatly improve the battery capability to attain the theoretical capacity. Researchers attributed this to the inconsistency of the heated carbon, and it was suggested that graphene be used as a coating in the future. Graphene has an anisotropic crystalline structure, making it a more consistent material than sucrose.

In this project, we studied the effect that carbon coating with graphene has on the performance of Li_2MSiO_4 cathode materials with equal ratios of Fe and Mn . We synthesized the $\text{Li}_2\text{Fe}_{0.5}\text{Mn}_{0.5}\text{SiO}_4$ cathode materials and tested the performance without the coating for comparison. We coated the lithium silicate nanomaterials with graphene, which we synthesized using physical vapor deposition. The composites were characterized through several tests. These included using scanning electron microscopy to verify the proper production of the batteries, and x-ray diffraction to characterize the composition of the synthesized materials.

We also tested the assembled coin cell's initial capacity and cycling life performance at a discharge/recharge rate of 0.1C for 20 cycles to determine the realized effectiveness of the graphene coating. Our results showed that the graphene coating greatly improved the discharge capacity of the lithium silicate batteries, while achieving exceptional current efficiency quickly. This makes graphene coated $\text{Li}_2\text{Fe}_{0.5}\text{Mn}_{0.5}\text{SiO}_4$ cathode materials a promising advance in energy storage.

1 Introduction

As we become more aware of carbon footprints and environmental issues surrounding non-renewable energy use, we become more dependent on technology to provide us with reliable and environmentally sound energy sources. As technologies, including power derived from solar energy, wind, water, hydrogen, and biofuels are developed, it becomes increasingly important that we are able to store this energy in an efficient, cost-effective way. Battery technology, therefore, is vital to our technological advancement for sustainability.

Lithium-ion batteries are some of the most promising energy storage devices that exist today. They are widely used in technology today due to the high specific energies, high energy density, and long cycle life. In current applications, such as powering hand-held electronics and other, small-scale devices, lithium-ion batteries are very successful. However, as we move to introduce these batteries into larger applications, such as electric vehicles and energy storage units for renewable resources, the need for rate capability and longer life cycle becomes increasingly important.¹ In order for these advancements to be made, further development and improvement of lithium-ion battery technology is essential.

Lithium-ion battery research and development has been a significant focus in many laboratories and research projects. Researchers have studied various materials for application in all parts of lithium-ion batteries. Some technologies utilize nanomaterials such as carbon nanotubes and others have involved the development of especially conductive polymers.^{2,3} Each development has made improvements on the capacity, cycle ability, performance, or cost-effectiveness. Most of these technologies are still in

¹ Zhang, P. "Structural properties and energetics of Li₂FeSiO₄ polymorphs and the delithiated products from first-principles." *PubMed* 14.20 (2012): *National Center for Biotechnology Information*. Web. 24 Sept. 2012. <<http://pubs.rsc.org/en/content/articlepdf/2012/cp/c2cp40811b>>.

² Bullis, Kevin. "A Guide to Recent Battery Advances." *Technology Review*. N.p., 29 June 2010. Web. 1 Sept. 2012. <<http://www.technologyreview.com/news/419591/a-guide-to-recent-battery-advances/>>.

³ Preuss, Paul. "Better Lithium-Ion Batteries Are On The Way From Berkeley Lab." *Berkeley Lab*. N.p., 23 Sept. 2011. Web. 1 Sept. 2012. <<http://newscenter.lbl.gov/news-releases/2011/09/23/better-li-ion-batteries/>>.

the research and development phase and these new ideas often bring forth new problems. Therefore, the market is always open for new lithium-ion battery advancements.

Lithium silicates are a promising material for lithium-ion battery cathodes as they have a high theoretical capacity with two lithium atoms per molecule, rather than only one as in conventional cathode materials. A 2012 Major Qualifying Project team worked to develop and test such cathode materials. The team determined that a cathode material composed of two lithium silicates, $\text{Li}_2\text{FeSiO}_4$ and $\text{Li}_2\text{MnSiO}_4$, in equal proportions would increase the initial capacity and cycling ability of the battery.⁴ The results were promising, but required more work for further advancement. Namely, the lithium silicates require a uniformly distributed, conductive coating in order to achieve the theoretical capacity, as the silicates are not conductive on their own. Graphene, a form of carbon that exists in nano-sized sheets, is a good candidate for this application due to its highly crystalline structure and small size, which theoretically would enable even distribution throughout the cathode.

The goal of this project was to explore the synthesis of graphene and analyze the effect of a graphene coating on the performance of batteries composed of $\text{Li}_2\text{Fe}_{0.5}\text{Mn}_{0.5}\text{SiO}_4$ cathodes. Our team synthesized both the graphene and the cathode precursor material, coated the cathode precursor with the graphene, and completed the reaction to create the final $\text{Li}_2\text{Fe}_{0.5}\text{Mn}_{0.5}\text{SiO}_4/\text{C}$ composite. We also synthesized non-coated $\text{Li}_2\text{Fe}_{0.5}\text{Mn}_{0.5}\text{SiO}_4$ cathodes for comparison. We then characterized the synthesized materials through scanning electron microscopy (SEM), energy dispersive x-ray spectroscopy analysis (EDX), and x-ray diffraction (XRD). We then assembled coin

⁴ Boucher, Andrew, Michael Ducey, and Nathan McNeff. "Synthesis, Characterization and Electrochemical Performance of $\text{Li}_2\text{FexMn}_{1-x}\text{SiO}_4/\text{C}$ as Cathode Material for Thin-Film Lithium-Ion Batteries." Diss. Worcester Polytechnic Institute, 2012. May 2012. Web. <http://www.wpi.edu/Pubs/E-project/Available/E-project-042512-143718/unrestricted/Synthesis,_Characterization_and_Electrochemical_Performance_of_Li2FexMn1-xSiO4_Cathode_Material_for_Thin-Film_Lithium-Ion_Batteries.pdf>.

cell batteries and performed electrochemical analysis to evaluate the discharge capacity and current efficiency of the batteries.

In this paper, we will begin by discussing the relevance and background to our project, the lithium silicates and graphene materials that we used in our batteries, and materials characterization. We will then detail the procedures we followed to synthesize and test graphene and $\text{Li}_2\text{Fe}_{0.5}\text{Mn}_{0.5}\text{SiO}_4$ cathode materials. Next, we will show and discuss the results of our experiments. Finally, we will make conclusions based on our results and provide recommendations for continuing the work on this iterative project.

2 Literature Review

This chapter provides background information relevant to the production and analysis of lithium-ion batteries. The history of lithium-ion batteries is first discussed along with the future prospects and how present day lithium-ion batteries function. The key findings from the previous MQP are then summarized; and the cathode materials that we synthesized, $\text{Li}_2\text{FeSiO}_4$ and $\text{Li}_2\text{MnSiO}_4$, are discussed. Information on the synthesis of graphene, as well as the process of carbon coating, will be provided. Finally, different methods for characterizing the synthesized battery materials and capacity testing are described.

2.1 Li-Ion Batteries Background

In response to the need for more efficient batteries, the lithium-ion battery was conceived and developed in Japan by Asahi Kasei Co. and first commercialized by Sony Co. in 1991.⁵ Other companies quickly followed suit, and the lithium-ion battery was soon powering consumer products such as cellular telephones, cameras, notebook computers, and other portable electronics. The lithium-ion battery was ideal because of its high energy density, cycling ability, and retention of charge memory, which was a problem that occurred with nickel-cadmium (Ni-Cd) and nickel-hydride (Ni-MH) batteries.⁶ Furthermore, the self-discharge rate of lithium-ion batteries is less than half of the Ni-Cd and Ni-MH batteries.⁷ Lithium is the lightest of all metals, has the greatest electrochemical potential, and provides the largest energy content.⁸ This allows the lithium-ion battery to provide the same amount of energy in a smaller, more lightweight package than the competing technologies.

⁵ Brodd, Ralph J. "Synopsis of Lithium-Ion Battery Markets." *Lithium-Ion Batteries*. New York: Springer, 2009. 1-7. *Springerlink*. Web. 18 Sept. 2012. <<http://www.springerlink.com/content/978-0-387-34444-7/#section=738165&page=1&locus=0>>.

⁶ Brodd, Ralph J. "Introduction: Development of Lithium-Ion Batteries." Introduction. *Lithium-Ion Batteries*. By Masaki Yoshio and Akiya Kozawa. New York: Springer, 2009. xvii-xv. *SpringerLink*. Springer Science Business Media. Web. 18 Sept. 2012. <<http://www.springerlink.com/content/978-0-387-34444-7/#section=738164&page=22&locus=58>>.

⁷ Buchmann, Isidor. "Will Lithium-Ion Batteries Power the New Millennium?" *Batteries in a Portable World*. Cadex Electronics Inc., Apr. 2001. Web. 18 Sept. 2012. <<http://www.buchmann.ca/Article5-Page1.asp>>.

⁸ *Ibid.*

The lithium-ion battery has seen great improvements in performance since it was first developed. Sony's original version used a coal product, referred to as coke, as the negative electrode, but since 1997, most lithium-ion batteries now use graphite. Using graphite as the anode instead of coke provides a flatter discharge voltage curve, followed by a rapid voltage drop before the discharge cut off.⁹ Figure 2-1 depicts this difference in the two materials.

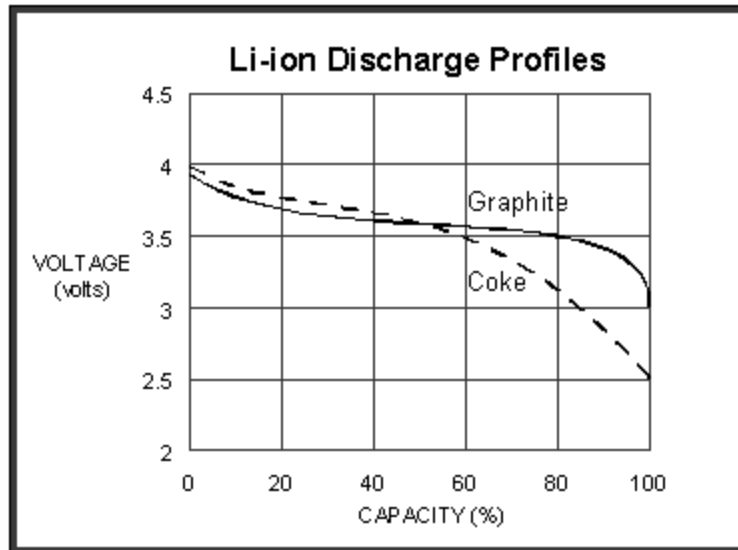


Figure 2-1: Li-Ion Battery Discharge Characteristics.¹⁰

There are several, different cathode materials that have been created for use in lithium-ion batteries. The most popular cathode material in lithium-ion batteries is LiCoO_2 , but materials such as LiMn_2O_4 and LiFePO_4 , among others, have also been developed. The best cathode material to use depends on the desired function of the battery and the type of product the battery is going to power.

Between 1991 and 2006, the sales and production of lithium-ion batteries experienced double-digit growth. Over this period, the energy density of the battery cell more than doubled, while the price fell by 50 percent.¹¹ With continued research being

⁹ Ibid.

¹⁰ Ibid.

¹¹ Brodd, Ralph J. "Synopsis of Lithium-Ion Battery Markets." *Lithium-Ion Batteries*. New York: Springer, 2009. 1-7. Springerlink. Web. 18 Sept. 2012. <<http://www.springerlink.com/content/978-0-387-34444-7/#section=738165&page=1&locus=0>>.

done to improve lithium-ion battery electrode and electrolyte materials, the push for creating superior, safe, high-performance batteries will continue to increase and make a presence in the consumer, medical, and industrial markets.

2.2 Future of Lithium-Ion Batteries

While the lithium-ion battery technology shows increasing promise, the advancement of technology necessitates that the batteries improve in several areas. The prospect of batteries as a significant facilitator in more efficient and sustainable technology is barred by the capabilities of today's batteries. In order to move towards such technological advancement, batteries are needed that can store greater amounts of energy, deliver that energy faster and more reliably to the technology being powered, and be more cost effective than they are today.¹² Additionally, lithium-ion batteries typically experience reduced capacity after one year, even if they are not consistently in use, and they usually fail after two to three years.¹³ Electric cars are an example frequently used to demonstrate the need for superior batteries. Hybrid cars utilize the battery to drive the car at low speeds, facilitate acceleration, and capture energy that would be lost as heat when the car is braking.¹⁴ This technology has been improved dramatically, but limitations on the capabilities of the materials, namely anode capacity, have prevented the improvement and increased production of fully electric vehicles. Current batteries do not allow fully electric vehicles to travel far before needing to be recharged, a task that can take several hours to complete.

Despite these obstacles, the potential for lithium-ion batteries remains quite good. There are numerous developments in the research for improvement of lithium-ion batteries. These include lithium-ion batteries that utilize carbon nanotubes, batteries in which an electrode interfaces with air, and batteries which make use of

¹² Bullis, Kevin. "A Guide to Recent Battery Advances." Technology Review. N.p., 29 June 2010. Web. 1 Sept. 2012. <<http://www.technologyreview.com/news/419591/a-guide-to-recent-battery-advances/>>.

¹³ "Is Lithium-ion the Ideal Battery?" Battery University. N.p., n.d. Web. 1 Sept. 2012. <http://batteryuniversity.com/learn/article/is_lithium_ion_the_ideal_battery>.

¹⁴ Bullis, Kevin. "A Guide to Recent Battery Advances." Technology Review. N.p., 29 June 2010. Web. 1 Sept. 2012. <<http://www.technologyreview.com/news/419591/a-guide-to-recent-battery-advances/>>.

special polymers to overcome various other obstacles posed by current technology.^{15,16} Each new technology makes some-possibly-significant improvement on the cycle ability, performance, or chargeability, while also focusing on the overall cost-effectiveness. Our goal is to contribute additional research data to help further develop the current lithium-ion technology.

2.3 Lithium-Ion Battery Mechanism

A battery is a device consisting of a group of electrochemical cells that converts chemical energy into electrical energy (Merriam-Webster, 2012). There are two main types of batteries: primary batteries and secondary batteries. Primary batteries, such as alkaline or carbon-zinc, are designed to be used only once, and are not rechargeable. Secondary batteries are able to be discharged and recharged many times throughout their life-span. Figure 2-2 compares the properties of several of today's most promising battery technologies.¹⁷ Lithium-ion batteries are one of the most promising examples of secondary batteries.

¹⁵ Ibid.

¹⁶ Preuss, Paul. "Better Lithium-Ion Batteries Are On The Way From Berkeley Lab." Berkeley Lab. N.p., 23 Sept. 2011. Web. 1 Sept. 2012. <<http://newscenter.lbl.gov/news-releases/2011/09/23/better-li-ion-batteries/>>.

¹⁷ Riezenman, Michael J., ed. "The Search For Better Batteries." *IEEE Spectrum* (1995): 51-56. *IEEE Xplore*. IEEE. Web. 18 Sept. 2012. <<http://ieeexplore.ieee.org/stamp/stamp.jsp?tp=>>>.

Cell type	Nominal voltage, V	Specific energy, Wh/kg	Energy density, Wh/L	Specific power, W/kg	Power density, W/L	Self-discharge, %/month	Cycle life ^a	Comments
Alkaline ^b	1.5	150	375	14	35	0.3	1	Not rechargeable
Lead-acid	2.0	35	70	~200	~400	4-8	250-500	Least-cost technology
Lithium-ion	3.6 ^c	115	260	200-250	400-500	5-10	500-1000	Intrinsically safe; contains no metallic lithium
Lithium-polymer ^d	3.0	100-200	150-350	>200 ^e	>350 ^e	~1	200-1000	Not yet available commercially; contains metallic lithium
Nickel-cadmium	1.2	40-60	60-100	140-220	220-360	10-20	300-700	Exhibits memory effect
Nickel-metal hydride ^f	1.2	60	220	130	475	30	300-600	May exhibit slight memory effect—experts disagree
Zinc-air ^g	1.2	146	204	150	190	~5	~200	Requires air manager to limit self-discharge

^a Very broad ranges are shown because cycle life is strongly dependent on how the battery is treated.

^b Data on the popular Duracell alkaline D cell is included just to put rechargeable batteries in perspective.

^c Li-ion cells with petroleum coke anodes drop from about 4.0 to about 3.0 V, in fairly linear fashion as they go from fully charged to fully discharged.

^d Since commercial units are at least a year away, these figures are only predictive.

^e These power figures apply at full charge; they will drop considerably as the cell discharges.

^f Ni-MH data applies to 2.9-Ah 4/3 A cells, of the kind made by Duracell and Toshiba.

^g Zinc-air data is for the cell that Zinc-Air Power is about to use in a prototype battery for electric vehicles.

▲ For all their seeming hardness, these figures give at best a rough notion of how the technologies compare. Truly comparable cells are not made in every technology. The data was not obtained under identical conditions from all cell types. Note also that data on specific energy and specific power may not always apply to the same device, since cell designs may maximize one at the expense of the other.

Figure 2-2: A table comparing the most promising batteries of today's market.¹⁸

Each electrochemical cell within a typical lithium-ion battery contains four major components; the anode, cathode, electrolyte, and separator. The anode is a porous negative electrode and serves as the negative terminal of the cell. It is typically made of graphite or petroleum coke. The cathode is a porous positive electrode and serves as the positive terminal of the cell. The cathode can have different chemistries, but is most commonly a metal oxide or a blend of multiple metal oxides. The electrolyte is a concentrated solution that has charged species that can move in response to an electrochemical potential and allow ions to travel between electrodes. A separator is a thin porous, non-conductive medium that physically insulates the negative from the positive electrode and prevents electrons from flowing freely between the electrodes. However, since it is porous, it does allow lithium-ions to pass through it via the

¹⁸ Ibid.

electrolyte.¹⁹ Figure 2-3 shows a cross section of a typical thin-film lithium-ion battery cell.

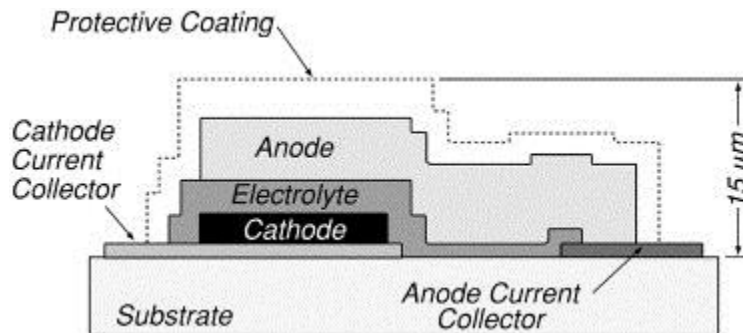


Figure 2-3: Schematic cross-section of a thin-film lithium battery.²⁰

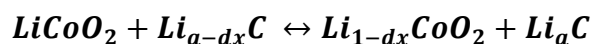
Batteries operate and create electrical current through a reduction-oxidation reaction, also known as a redox reaction. When the anode and cathode of the battery are connected by an electrical conductor, such as a wire, electrons will flow from the battery's anode through the wire to the cathode, creating an electrical current. This occurs because the anode undergoes a chemical reaction with the electrolyte in which the electrolyte extracts a positive ion, or cation, a +1 cation in the case of lithium. This causes a negatively charged particle, an electron, to travel through the wire to the cathode. This is the oxidation half of the reaction. The lithium-ion passes through the separator via the electrolyte and reacts with the cathode at its surface, reducing it back to its non-charged state. This is the reduction half of the reaction. The most commonly used cathode material in lithium-ion batteries today is lithium cobalt oxide. For this material, the chemical reaction that occurs at the cathode surface is:



¹⁹ Chaturvedi, Nalin A., Reinhardt Klein, Jake Christensen, Jasim Ahmed, and Aleksander Kojic. "Modeling, Estimation, and Control Challenges for Lithium-ion Batteries." *IEEE Xplore*. Proc. of 2010 American Control Conference, Marriott Waterfront, Baltimore, MD. N.p., n.d. Web. 18 Sept. 2012. <<http://ieeexplore.ieee.org/stamp/stamp.jsp?tp=>>.

²⁰ N.J. Dudney, B.J. Neudecker. "Solid state thin-film lithium battery systems, Current Opinion". *Solid State and Materials Science*, Volume 4, Issue 5, October 1999, Pages 479-482, ISSN 1359-0286, 10.1016/S1359-0286(99)00052-2.

The overall reaction, in the case of a lithium cobalt oxide/graphite system, is the following:



The electrons travel through the wire from anode to cathode in an attempt to reach equilibrium in the battery. Since there is a higher energy in the anode than in the cathode, the electrons travel from the anode to the cathode. The battery is fully discharged once it reaches equilibrium, and must be recharged by putting electrical energy in, causing the reaction to run in reverse and the lithium ions to migrate back over to be stored in the anode.²¹

The electrodes in a lithium-ion cell are both made from intercalation materials. Intercalation materials are materials that have a lattice structure into which a guest species, such as lithium ions, may be inserted and extracted without significant structural modification of the host material.²² Lithium-ion battery electrode materials can have either a layered structure or a spinel structure. A material with a layered structure, such as $LiCoO_2$, allows for the two-dimensional diffusion of the lithium-ion. A material with a spinel structure, such as $LiMn_2O_4$, enables three-dimensional diffusion of the lithium-ion within the electrode material.²³ Figures 2-4 and 2-5 show the layered structure of $LiCoO_2$ and the spinel structure of $LiMn_2O_4$, respectively.

²¹ "Lithium-ion Batteries." *Physics Central*. American Physical Society, n.d. Web. 18 Sept. 2012. <<http://www.physicscentral.com/explore/action/lithium-1.cfm>>.

²² Riezenman, Michael J., ed. "The Search For Better Batteries." *IEEE Spectrum* (1995): 51-56. *IEEE Xplore*. IEEE. Web. 18 Sept. 2012. <<http://ieeexplore.ieee.org/stamp/stamp.jsp?tp=>>>.

²³ Yoshio, Masaki, and Hideyuki Noguchi. "A Review of Positive Electrode Materials for Lithium-Ion Batteries." *Lithium-Ion Batteries*. New York: Springer, 2009. 9-48. *SpringerLink*. Springer Science Business Media. Web. 18 Sept. 2012. <<http://www.springerlink.com/content/978-0-387-34444-7/>>>.

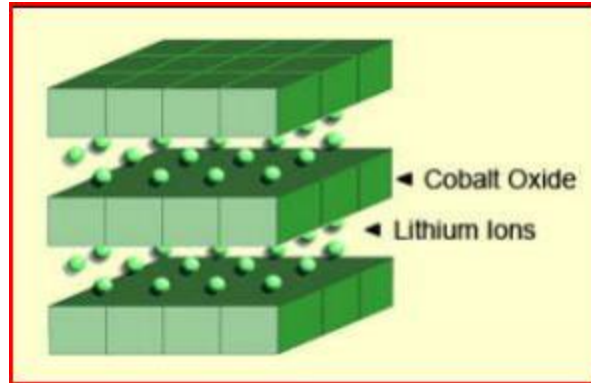


Figure 2-4: Layered structure of lithium cobalt oxide.²⁴

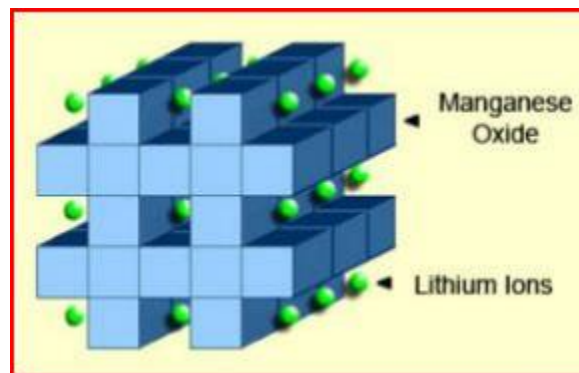


Figure 2-5: Spinel structure of lithium manganese oxide.²⁵

A significant factor in how much power can be exerted by the lithium-ion battery depends on the contact area between the electrode and the electrolyte. A larger contact area leads to a greater transfer of ions, and thus more power. To take advantage of this fact, thin-film lithium-ion batteries have been developed in order to maximize the surface area of the electrodes that come in contact with the electrolyte.

2.4 Lithium Silicate Materials

In this project, we studied a dual-phase lithium silicate material because of the enhancing capabilities to improve the superior performance aspects of each, individual

²⁴ Boucher, Andrew, Michael Ducey, and Nathan McNeff. "Synthesis, Characterization and Electrochemical Performance of $\text{Li}_2\text{FexMn}_{1-x}\text{SiO}_4/\text{C}$ as Cathode Material for Thin-Film Lithium-Ion Batteries." Diss. Worcester Polytechnic Institute, 2012. May 2012. Web. <http://www.wpi.edu/Pubs/E-project/Available/E-project-042512-143718/unrestricted/Synthesis,_Characterization_and_Electrochemical_Performance_of_Li2FexMn1-xSiO4_Cathode_Material_for_Thin-Film_Lithium-Ion_Batteries.pdf>.

²⁵ Ibid.

material. We will discuss the iron silicate and the role of polymorphs, as well as the manganese silicate.

2.4.1 $\text{Li}_2\text{FeSiO}_4$ Polymorphs

Polymorphism in materials science is the capability of a crystalline material to exist in more than one crystal structure. Polymorphism can potentially be found in many crystalline materials, including polymers, minerals, and metals. The complete morphology of a material is described by polymorphism and other variants, including crystal tendencies and crystallographic defects.²⁶

When polymorphism is a result of a difference in crystal packing, it is called packing polymorphism. Polymorphism can also be caused by the existence of different conformers of the same molecule in conformational polymorphism. In pseudo-polymorphism, the different crystal types are the result of hydration or solvation. Silica is known to form many polymorphs. Polymorphs have different stabilities and may spontaneously convert from an unstable form to a stable form at a particular temperature. They also exhibit different melting points and solubilities, x-ray crystal and diffraction patterns. Various conditions in the crystallization process are responsible for the development of different polymorphic forms. These conditions include:

- solvent effects (the packing of crystals may be different in polar and nonpolar solvents);
- certain impurities inhibiting growth pattern and favoring the growth of a metastable polymorph;
- the level of supersaturation from which a material is crystallized (generally: the higher the concentration above the solubility, the more likelihood of metastable formation);
- temperature at which crystallization is carried out;

²⁶ Kalpakjian, Serope. *Manufacturing Engineering and Technology*. 6th ed. Reading, MA: Addison-Wesley, 1989. 43. Print.

- geometry of covalent bonds (differences leading to conformational polymorphism); and
- modifications in stirring conditions.²⁷

A study by Zhang *et al.* reported structures of $\text{Li}_2\text{FeSiO}_4$ polymorphs and the influence on structural stability and equilibrium voltage. $\text{Li}_2\text{FeSiO}_4$ can adopt several crystalline structures, related to high- and low-temperature polymorphs of Li_3PO_4 . In the experiment, Zhang *et al.* studied the structural characteristics, the stabilities and the electrochemical properties of the three $\text{Li}_2\text{FeSiO}_4$ polymorphs crystallizing in the space groups $\text{Pmn}2_1$, $\text{P}2_1/\text{n}$, and Pmnb as seen in Figure 2-6 below. The results demonstrate that the differences in the local environments around a given FeO_4 tetrahedron immediately translated into varying degrees of distortion of FeO_4 that influenced the structural stability and the equilibrium voltage in all $\text{Li}_2\text{FeSiO}_4$ polymorphs. Moreover, a higher degree of distortion of FeO_4 tetrahedron results in lower structural stability, and a polymorph with more stable $\text{Li}_2\text{FeSiO}_4$ structure and less stable LiFeSiO_4 structure has been shown to output a higher voltage. Alternatively, the bonding characteristics of Si–O remain almost unchanged during the lithiation–delithiation process for all the polymorphs. The strong Si–O bonds contribute significantly to the structural stability during the lithium transfer. Furthermore, $\text{Li}_2\text{FeSiO}_4$ has the possibility of extracting more than one lithium-ion per formula unit for $\text{P}2_1/\text{n}$ polymorph. The $\text{P}2_1/\text{n}$ structure, which shows a small volume change and small voltage increase between the first and second voltage steps, may be a possibility for the further extraction of part of the second lithium-ion in $\text{Li}_2\text{FeSiO}_4$.²⁸

²⁷ Kalpakjian, Serope. *Manufacturing Engineering and Technology*. 6th ed. Reading, MA: Addison-Wesley, 1989. 43. Print.

²⁸ Zhang, P. "Structural properties and energetics of $\text{Li}_2\text{FeSiO}_4$ polymorphs and the delithiated products from first-principles." *PubMed* 14.20 (2012): *National Center for Biotechnology Information*. Web. 24 Sept. 2012. < <http://pubs.rsc.org/en/content/articlepdf/2012/cp/c2cp40811b>>.

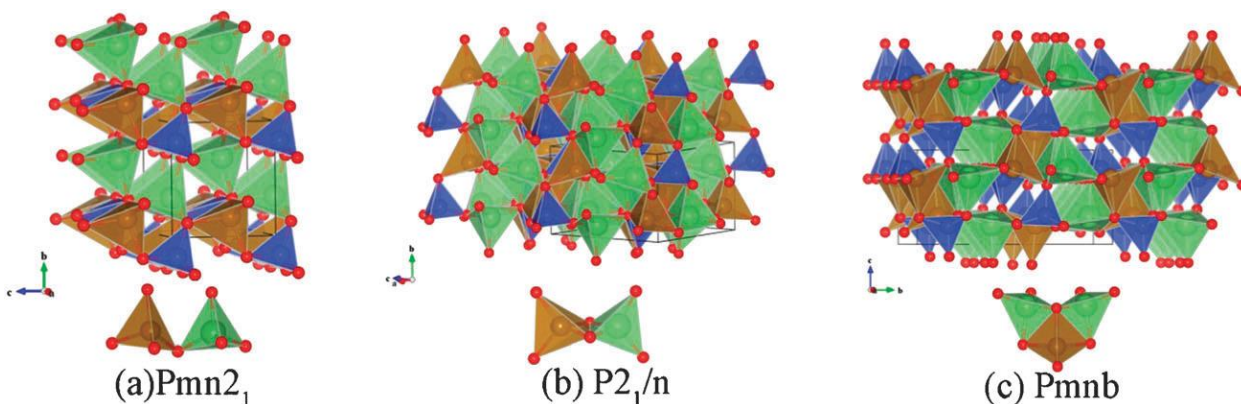


Figure 2-6: Polymorphs in the space groups (a) $Pmn2_1$, (b) $P2_1/n$, and (c) $Pmnb$.²⁹

Structural properties, thermodynamic stability and the removal process of lithium ions for Li_2FeSiO_4 polymorphs were studied using density functional theory (DFT). The differences in local environment around FeO_4 tetrahedra were moved into varying degrees of distortion, which showed a significant influence on the structural stability and average voltages. Figure 2-7 shows how the changing structure of the polymorphs affected the voltage output. Zhang *et al.* demonstrated that the strong Si–O bonds remain almost unchanged during the lithiation–delithiation process for all the polymorphs, which contribute significantly to the structural stability. These bonds are a major factor in the structural stability of the molecule during the process.³⁰

²⁹ Ibid.

³⁰ Ibid.

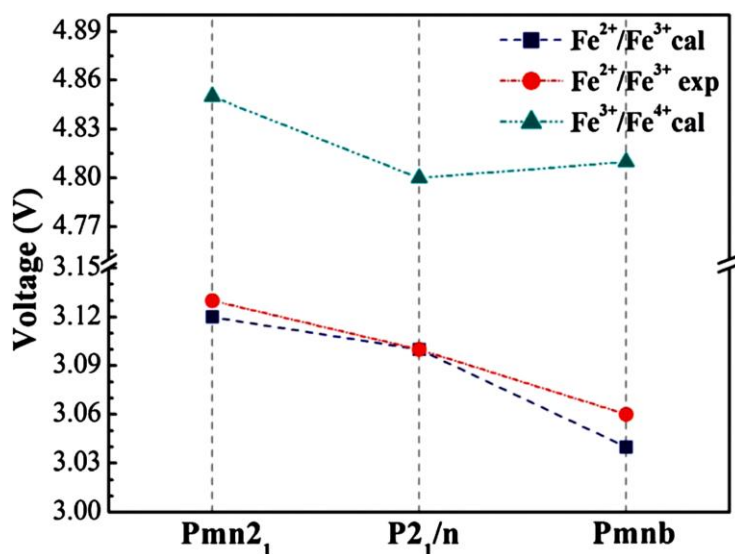


Figure 2-7: Performance of various polymorphs.

2.4.2 Li₂MnSiO₄

Several materials have opened a completely new possibility for cathode materials for lithium-ion batteries. In particular, LiFePO₄ has gained a lot of attention and, although it possesses a very low intrinsic conductivity, different preparation techniques have enabled the use of this material at extremely high C-rates, which we will discuss later on. There have also been other promising materials; most recently, Nyten *et al.* have reported preparation and basic characterization of the first member of silicate branch of Fe-based materials: Li₂FeSiO₄. This cathode material possesses the same benefits as LiFePO₄, with one major difference: two lithium-ions in the structure. The addition of the second lithium ion theoretically enables the exchange of two electrons per transition metal with a theoretical capacity of approximately 320 mAh g⁻¹ as seen in Figure 2-8. However, the electrochemical tests have shown that, within the electrolyte stability potential window, only up to 1 mol of lithium can be reversibly exchanged. The exchange of Fe with Mn leads to an isostructural material with a higher expected working voltage and with a possibility to obtain a cathode material where a

two-electron reaction (exploiting the MnII/MnIII and MnIII/MnIV redox pairs) becomes feasible.³¹

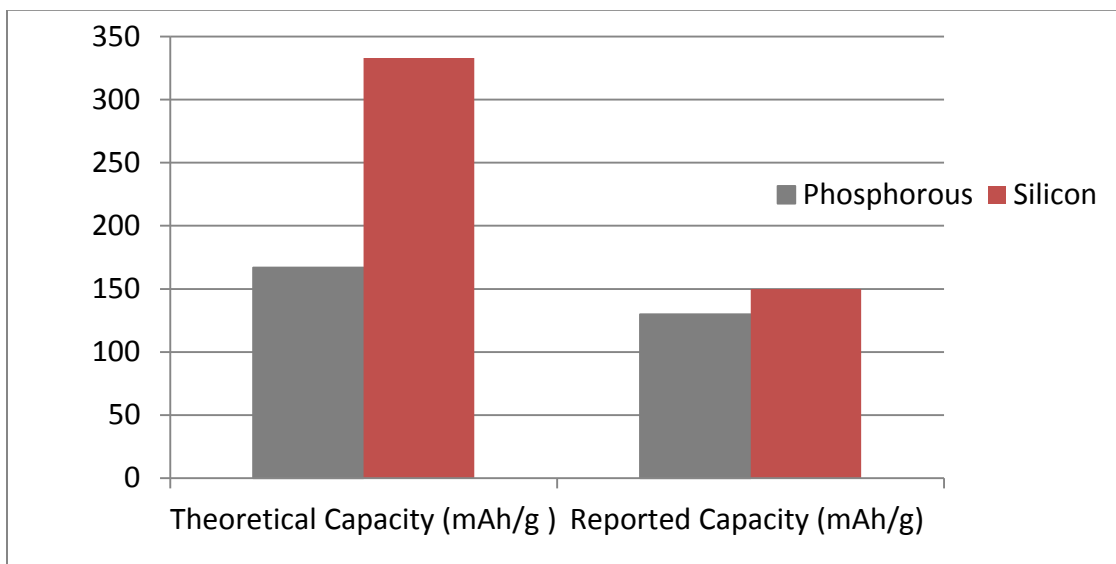


Figure 2-8: Data comparing the lithium phosphate and lithium silicate performances.

Dominko's group recently reported on the synthesis and first electrochemical characterization of $\text{Li}_2\text{MnSiO}_4$. Although it was clearly shown that the material could be cycled, the amount of reversibly exchanged lithium was relatively small (0.7 Li per formula unit, at most), while the irreversible losses, especially in the first cycles, were very large. Serious reversible capacity fading was observed.³² In that preliminary study, Dominko's group was not able to conclude whether the observed properties were due to inherent thermodynamic properties of $\text{Li}_2\text{MnSiO}_4$ or to kinetic problems caused by the low conductivity of silicates. However, it is well-known from the extensive work on olivines that the kinetic problems can be overcome by preparing very small active particles (a few tenths of nanometers in diameter) and embedding them into an electron conducting phase, such as a carbon coating or a carbon network.³³

³¹ Dominko, R. "Li₂MnSiO₄ as a potential Li-battery cathode material." *Journal of Power Sources* 174.2 (2007): 457-461. Print.

³² Ibid.

³³ Ibid.

Neither reduction of particle size nor increased carbon content (and optimized carbon distribution) has significantly improved the electrochemical performance of $\text{Li}_2\text{MnSiO}_4$. The polarization resistance decreased by merely 20mV and the capacity increased by 20 mAh g^{-1} to reach a maximum of about 140 mAh g^{-1} . The cycling stability has remained poor (about 4 mAh g^{-1} are lost per cycle). Obviously, the strategy that has proven extremely efficient in the case of LiFePO_4 , does not work in the case of $\text{Li}_2\text{MnSiO}_4$. Based on x-ray diffraction measurements of partially charged samples, Dominko speculated that extraction of Li leads to a progressive collapse of the initial structure. It was suggested that in a future study, one should focus primarily on the structural stabilization of $\text{Li}_2\text{MnSiO}_4$ rather than on improvement of electronic/ionic transport.³⁴

2.5 2012 MQP: Synthesis, Characterization and Electrochemical Performance of $\text{Li}_2\text{Fe}_x\text{Mn}_{1-x}\text{SiO}_4/\text{C}$ as Cathode Material for Thin-Film Lithium-Ion Batteries

The 2012 MQP team's goal was "to develop and test different cathode materials for lithium-ion batteries."³⁵ In the project, the team determined that lithium silicate compounds would have a higher capacity than non-silicate compounds because of the second lithium atom in each molecule. In order to find the compound with the best initial capacity and cycling ability of $\text{Li}_2\text{FeSiO}_4$ and $\text{Li}_2\text{MnSiO}_4$ in varying ratios, the team synthesized a cathode material of the two. The use of silicate, which is not very conductive, required a carbon-coat on the cathode in order to increase the conductivity and capacity of the material. Commercial sucrose was used as the carbon source.

Experiments determined that a ratio of 0.5:0.5 of $\text{Li}_2\text{FeSiO}_4$ to $\text{Li}_2\text{MnSiO}_4$ was the most successful sample in the project and would have the most potential for future

³⁴ Ibid.

³⁵ Boucher, Andrew, Michael Ducey, and Nathan McNeff. "Synthesis, Characterization and Electrochemical Performance of $\text{Li}_2\text{Fe}_x\text{Mn}_{1-x}\text{SiO}_4/\text{C}$ as Cathode Material for Thin-Film Lithium-Ion Batteries." Diss. Worcester Polytechnic Institute, 2012. May 2012. Web. <http://www.wpi.edu/Pubs/E-project/Available/E-project-042512-143718/unrestricted/Synthesis,_Characterization_and_Electrochemical_Performance_of_Li2FexMn1-xSiO4_Cathode_Material_for_Thin-Film_Lithium-Ion_Batteries.pdf>.

experiments.³⁶ While the carbon coating significantly increased the cycling ability of the cathode samples, it also greatly reduced the capacity. It was found that 10 weight percent carbon coated samples had the best electrochemical results, increasing conductivity, yet not decreasing the capacity as greatly as other samples.³⁷ The MQP team suggested utilizing graphene as a carbon coating, which would potentially be more effective than commercial sucrose due to its highly crystalline structure and ability to be present as nanoparticles. Additional research by a WPI graduate student found that oxidation of the material had occurred, indicating that the entire fabrication process may need to be revisited. The 2012 MQP has paved the way for our project, which will aim to refine the processes used and obtain better overall results.

2.6 Graphene

Graphite consists of multiple layers of carbon atoms. A single layer, free of other layers, is called graphene; an essentially two-dimensional structure with a thickness of approximately 340 pm. Graphene is resistant to fracture and deformation, has a high thermal conductivity, and has a conduction band that touches its valence band. The electrical properties can therefore be influenced by adding various functional groups. Graphene can be prepared both by mechanically peeling away layers of graphite and by a variety of specialized techniques, including chemical vapor deposition on metal substrates, and sonication of colloidal suspensions of graphite oxide. There have been numerous potential applications of graphene proposed, including the use in energy storage materials.³⁸

There have been growing concerns over nanoparticles, the size of particles used in this project, and the effect on the macro world and the health of various populations. Nanoparticles can be easily absorbed through the skin, lungs, digestive tract, and even transferred into human cells. With evidence of the capability of nanoparticles to pollute

³⁶ Ibid.

³⁷ Ibid.

³⁸ Miessler, Garry. "Graphene." *Inorganic Chemistry*. 4th ed. Upper Saddle River: Pearson, 2011. 278-80. Print.

the air, water, and soil, research is expanding to discover the risks nanoparticles pose to humans and the environment.³⁹ With the increasingly common presence of graphene in the electronic world, it is no surprise that environmental effects of graphene are being studied. Chemists at Rice University studied the life cycle of graphene and its chemical interactions with the environment as it decomposes. The study showed that graphene is broken down by *Shewanella* bacteria and becomes stacks of carbon layers, known as graphite, which have proven to be environmentally benign.⁴⁰

2.7 Characterization

As part of the purpose of this project was to work with nanomaterials, it will be imperative to make use of various manners to view the material up close in order to take measurements and determine the compositions. In addition to qualifying and quantifying the synthesized cathode materials, they were tested to see whether the hypothesized performance improvements were met. For the aforementioned purposes, use of a scanning electron microscope, x-ray powder diffraction machine, and galvanic charge/discharge cycle test station were employed.

2.7.1 Scanning Electron Microscopy

This section serves as an overview for the means and mechanisms of scanning electron microscopy (SEM) for the reader to be able to carry out the practice of preparing and generating amplified images. This method of viewing nano-scale samples, which are too small to be visible to the naked eye, is non-destructive, which makes it invaluable to sensitive cathode materials⁴¹.

A scanning electron microscope works by emitting a beam of electrons over the surface of a conductive specimen within a vacuum chamber, row by row. The specimen then reflects what are known as “secondary electrons,” and there are a few manners in

³⁹ Kalpakjian, Serope. *Manufacturing Engineering and Technology*. 6th ed. Reading, MA: Addison-Wesley, 1989. 43. Print.

⁴⁰ Mahony, Melissa. “Graphene Goes Green.” Smartplanet.com. 27 Jul. 2010. Web. 10 Mar. 2013.

⁴¹ “Scanning Electron Microscopy.” *The Gale Encyclopedia of Science*. Ed. K. Lee Lerner and Brenda Wilmoth Lerner. 4th ed. Vol. 5. Detroit: Gale, 2008. 3807-3808. Gale Virtual Reference Library. Web. 27 Aug. 2012.

which an electron beam might interact with the surface of a specimen. Varying paths for electrons could include absorption by the specimen, backscattering, forming a secondary beam, elastic and inelastic scattering, the reflection of x-ray and light photons, as well as ultimate transmittal.⁴² The variance in electron beam interaction depends on the composition and surface topography of the specimen.

The structure of an electron microscope is columned so that a beam of electrons might be properly filtered down to a specimen. At the top of the microscope is an electron emitting source, commonly a lanthanum hexaboride or tungsten hairpin thermionic filament. Such sources are focused into a pyramidal tip and heated resistively to enable outer electrons to surmount the energy necessary to escape the materials' atoms. The emitted beam is between one and fifty micrometers with a brightness between ($5 \times 10^9 \text{ A/m}^2 \cdot \text{sr}$) and ($5 \times 10^8 \text{ A/m}^2 \cdot \text{sr}$) and must be re-focused and reflected through a number of chambers until it will reach the specimen. There are a few other variations, but another viable source is a field emission source with a high negative potential at the sharp tungsten tip to allow the flow of electrons in a narrower beam. Lower energy spread is ideal in all of the emission variations. It will be important to understand the emission source to better understand the potential reaction with the surface of the cathode samples.

Travelling the distance through the various openings of the condensing lenses in a column allows the electron beam to reconvene and focus more precisely on a particular beam spot. By utilizing magnetic forces that may allow the electron beam to spiral and converge, the lenses increase the angle of contact with the specimen's surface plane.⁴³

The method of generating an image is capturing the resulting electron deflections and assigning an RGB value on a grey scale to each corresponding pixel to be

⁴² Stokes, D. (2009). *Principles and Practice of Variable Pressure: Environmental Scanning Electron Microscopy (VP ESEM)*. Chichester, GBR: Wiley.

⁴³ Stokes, D. (2009). *Principles and Practice of Variable Pressure: Environmental Scanning Electron Microscopy (VP-ESEM)*. Chichester, GBR: Wiley.

projected on a screen.⁴⁴ The electron beam will scan left to right across a specimen along a specific row path until it has covered the entire surface and generated a complete image. The magnification is determined on a point-by-point basis in which the length of the display is divisible by the specimen length, though this ratio is independent of absolute measurement values, which is why scale measurement bars are present on screen images. Understanding this will help the team to operate the machine to determine the size of particles on the surface of cathode specimens.

There are some limitations to the SEM method in resolution, or image quality, especially as compared to the TEM, but there are benefits to ease of sample preparation. An SEM-generated image may not exceed a single nanometer, while the TEM images may be better a tenth of a nanometer. While the image quality may be worse, such detail is not necessary for the application in this project, where the team will need resolution only up to one nanometer. Sample preparation is also important, as SEM specimens may be whole centimeters in width and depth, compared to tens of nanometers for TEM images.⁴⁵

2.7.2 Energy Dispersive X-ray Spectroscopy Analysis (EDX)

EDX analysis is a technique used for identifying the elemental composition of a specimen. The EDX analysis system works as an integrated feature of a scanning electron microscope, and cannot operate on its own.⁴⁶ When the incident electron beam produced by the SEM hits the atoms of the sample, some of the electrons from the sample atoms are knocked off from the shells and emitted as secondary electrons. When these secondary electrons are emitted from the sample atoms, they leave a hole in their place within the electron shell. If this occurs within an inner electron shell, not the outermost shell of an atom, the atom is no longer in a stable state. In order to get

⁴⁴"Scanning Electron Microscopy." *The Gale Encyclopedia of Science*. Ed. K. Lee Lerner and Brenda Wilmoth Lerner. 4th ed. Vol. 5. Detroit: Gale, 2008. 3807-3808. Gale Virtual Reference Library. Web. 27 Aug. 2012.

⁴⁵ Stokes, D. (2009). *Principles and Practice of Variable Pressure: Environmental Scanning Electron Microscopy (VP-ESEM)*. Chichester, GBR: Wiley.

⁴⁶ "EDX Analysis and WDX Analysis." SiliconFarEast.com. 2004. Web. 30 Mar. 2013.

back to a stable state, an electron from a further shell of the atom will drop into the inner shell. However, because the outer shells are at a higher energy state, the atom must lose some energy in order to do this. The energy lost by the atoms is released in the form of x-rays.⁴⁷

The amount of energy that is released by the transferring electron depends on which shell it is transferring from, as well as which shell it is ending up in, and each element produces x-rays with unique wavelengths and amounts of energy depending on the shells involved. By measuring the amounts of energy present in the x-rays being released during exposure of the specimen to the electron beam of the SEM, the identity of the atom from which the x-ray was emitted can be established. An EDX spectrum displays peaks, which correspond to the energy levels for which the most x-rays have been detected. Each peak can be related to a single element. Further, the higher the peak in the spectrum, the more concentrated that specific element is within the specimen, or sample area, being analyzed.⁴⁸

2.7.3 X-ray Powder Diffraction (XRD)

With x-ray powder diffraction, one may determine crystalline phase and microstructure of a sample with both qualitative and quantitative data. One may also investigate the texture with reflectometry and microdiffraction.⁴⁹

From the diffraction pattern of a particular x-ray frequency directed at a finely ground powder, one may determine the composition and crystalline structure from known data on planar crystal spacings. A cathode ray tube, which consists of a heated filament in a vacuum tube, will emit x-rays of a fixed wavelength that will be realigned in a parallel fashion to strike the powdered specimen at various angles until the bent x-

⁴⁷ "How EDX Works." Seal Laboratories. Web. 30 Mar. 2013.

⁴⁸ "EDX Analysis and WDX Analysis." SiliconFarEast.com. 2004. Web. 30 Mar. 2013.

⁴⁹ "X-ray powder diffraction system." Spectroscopy June 2009: 47. General OneFile. Web. 30 Aug. 2012. http://go.galegroup.com/ps/i.do?id=GALE%7CA204135237&v=2.1&u=mlln_c_worpoly&it=r&p=ITOF&sw=w

rays reflecting off the specimen satisfy Bragg's Law.⁵⁰ Bragg's law is pertinent to x-ray diffraction because it relates the incident angle of a diffracted beam to the interplanar spacing of a crystalline structure through calculation using the known wavelength of incident x-rays. Reflected x-rays at an angle equal to that of the incident beam will align to form a single wave of greater amplitude, seen in Figure 2-9, that can be collected and measured to determine the composition of the specimen. Unless the incident angle of a reflected beam allows the peaks of beams to align, they will cancel out as seen in Figure 2-9, below.⁵¹

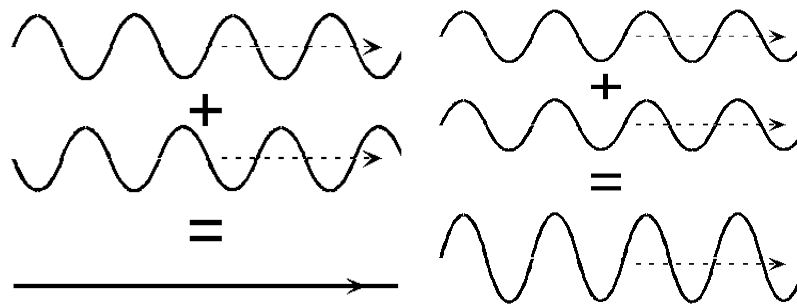


Figure 2-9: Destructive interface (left) and constructive interface (right) of XRD signals.⁵²

2.8 Electrochemical Testing

Of great importance to the potential users of a battery are some key characteristics: cycling ability, capacity, and self-discharge rates. In order to determine these criteria, a number of processes fall under the umbrella of electrochemical testing: constant voltage or current test cycles (galvano/potentiostatic cycling) and measures of internal impedance.⁵³

⁵⁰ Dutrow, Barbara L., and Christine M. Clark. "X-ray Powder Diffraction (XRD)." X-ray Powder Diffraction (XRD). Louisiana State University, Eastern Michigan University, n.d. Web. 7 Sept. 2012. <http://serc.carleton.edu/research_education/geochemsheets/techniques/XRD.html>.

⁵¹ Henry, Darrell, Nelson Eby, John Goodge, and David Mogk. "X-ray Reflection in Accordance with Bragg's Law." *BraggsLaw*. Louisiana State University, University of Massachusetts – Lowell, University of Minnesota – Duluth, Montana State University, n.d. Web. 7 Sept. 2012. <http://serc.carleton.edu/research_education/geochemsheets/BraggsLaw.html>.

⁵² Ibid.

⁵³ "Electrochemical Energy Sources." Lecture. Bulgarian Academy of Sciences, 2009. Web. 10 Sept. 2012. <<http://www.bas.bg/cleps/poemes/eschool/e-School%20Stoynov.pdf>>.

For this project, the team will need only to perform galvanostatic (constant current) cycling tests in order to derive the capacity and efficiency of the cathode material. To perform a nominal capacity test for charge/discharge cycles, one must prepare an electrolyte solution as well as an anode in order to facilitate the flow of electrons to gather data on the charge and subsequent discharge.⁵⁴ The C-rate is often used to describe battery loads or battery charging. 1C is the capacity rating of the battery measured in Amp-hours. The current applied must be in some constant measure of coulombs for ten to twenty hours or the charge/discharge period.

2.9 Summary

In order to carry out this project, we needed sufficient background information, which would both educate us and legitimize our work for the methodology. We have a firm grasp on the history, present technology, and future of lithium-ion batteries, which are the basis of our project. The composition and procedures by which we will go about creating our cathode materials are pertinent information, as well as having an understanding of our characterization and testing processes. Next, we will go into detail about our methods.

⁵⁴ Goia, Daniel Crain, Jianping Zheng, Christopher Sulyma, Corina Goia, Dan, and Dipankar Roy. "Electrochemical Features of Ball-milled Lithium Manganate Spinel for Rapid-charge Cathodes of Lithium-ion Batteries." *SpringerLink*. Springer Science Business Media, 22 Feb. 2012. Web. 12 Sept. 2012. <<http://www.springerlink.com/content/28225816v076w701/fulltext.html>>.

3 Methodology

The purpose of this chapter is to explain the steps taken to complete this study of the $\text{Li}_2\text{Fe}_{0.5}\text{Mn}_{0.5}\text{SiO}_4$ carbon-coated cathode material. Figure 3-1 below is a flowchart diagramming the steps that were taken during the process of completing this project, which involved synthesis of the lithium silicate and graphene, creating the final cathode composite, and assembling and testing the batteries.

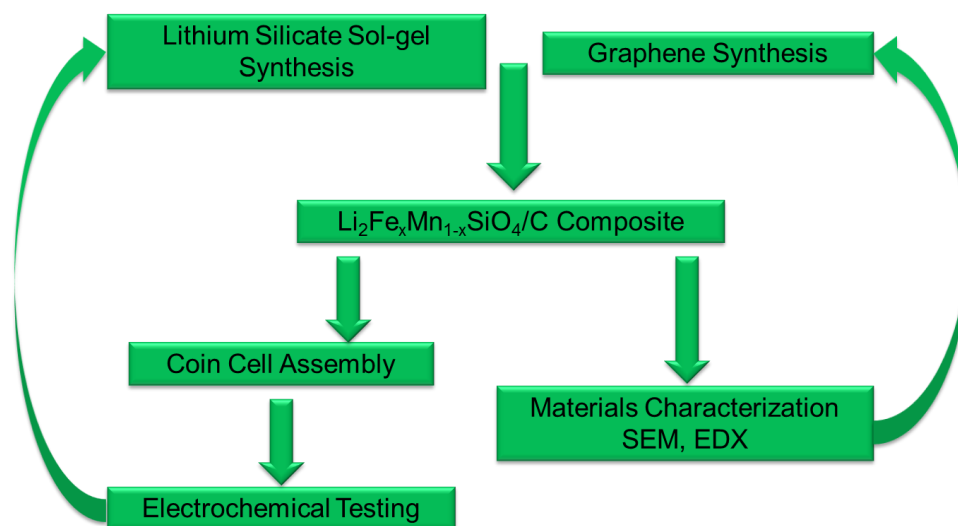


Figure 3-1: Flowchart of steps involved in the complete project process.

3.1 Synthesis of Cathode Precursor

The first step that had to be taken in the process of creating the coin cell batteries was the synthesis of the cathode precursor material, for which a sol-gel process was utilized. This process involved creating a gel composite solution in order to form a powder for carbon coating. To prepare the gel, 4.534 g of lithium acetate dihydrate (Alfa Aesar, 99%) was massed out and dissolved into 20 mL of ethanol. The solution was stirred for approximately 10 minutes while under a low-flow nitrogen flux. To this solution, the correct amounts of iron and manganese had to be added in order to yield the stoichiometric ratio that was desired for the gel.

First, 2.747 g of manganese acetate tetradihydrate (Alfa Aesar, Mn 22%) was massed out and added to the solution. Next, 1.9989 g of ferrous oxalate dihydrate (Alfa Aesar, 99%) was massed out and also added to the solution, which was still mixing under nitrogen flux. This step had to be done as quickly as possible, since the iron compound was highly reactive and oxidized readily with the atmosphere, which needed to be avoided. This lithium/manganese/iron solution was now left to mix under nitrogen flux while another, separate solution was made.

The other solution was created by first measuring out 5 mL of tetraethyl orthosilicate (Aldrich, Reagent Grade, 98%) and adding 1.5 mL of acetic acid to it. Next, 0.5 mL of deionized (DI) water was mixed in after which the solution was added dropwise to the lithium/manganese/iron solution. The acetic acid in the second solution acted as a catalyst, and allowed a hydrolysis reaction to occur between the tetraethyl orthosilicate (TEOS) and the water. This hydrolysis reaction allowed for a polymerization reaction to occur and for the gel to begin forming once the two solutions were mixed. This polymerization reaction yielded the molecular network desired with the formation of the gel. As the gel was forming, the mixture was left under a nitrogen flux and stirred via a magnetic stirring rod, set at 100 rpm, as shown in Figure 3-2. This mixing was allowed to go on for 12 hours.



Figure 3-2: Mixing of solution to form gel under nitrogen flux using stirring rod.

Once the gel was fully formed, it was taken out of the fume hood, scooped out of the flask, and placed into a ceramic boat, which could then be placed into the tube furnace (Thermolyne 79300). The furnace tube was already full of nitrogen when the ceramic boat containing the gel was placed inside, and the nitrogen flux continued to be run through the tube during and after the gel was properly positioned. The furnace was heated to 100°C at a rate of 3°C per minute. Once the furnace reached 100°C, it was kept there for 24 hours in order to completely dry out the gel. After all of the solvent had evaporated from the gel's pores, the dried composite was removed from the furnace and ceramic boat, and it was ground up using a ceramic mortar and pestle.

3.2 Synthesis of Active Cathode

At this point, the powder obtained from the dry gel was the cathode precursor material. The next step in the process was to carbon coat this material with graphene, for which the synthesis process is detailed below. The cathode precursor was taken and mechanically mixed with graphene in an 18 to 1 mass ratio. The correct masses of cathode precursor and graphene were placed into a ceramic mortar and ground with a pestle, after which the material was placed in a glass vial and allowed to sonicate (Branson 2510) for one hour. Now that the powder was evenly and uniformly mixed, it

was pressed into a pellet using a crimping machine (MSK-110) set at 2,000 psi for two minutes.

This pellet was then taken and placed into the tube furnace under a nitrogen flux in order to allow calcination to occur, as shown in Figure 3-3. In order to get the desired crystal structure, a heat rate of 10°C per minute until the furnace reached 300°C was used, after which the heat rate was changed to 2°C per minute until the furnace reached 700°C. Once at 700°C, the pellet was allowed to calcinate for 10 hours, after which the furnace was allowed to cool. Once cool, the pellet was removed from the furnace and from the nitrogen flux and ground into a fine powder with a mortar and pestle. This powder was the carbon coated active cathode material, which was used in the assembly of the coin-cell batteries.



Figure 3-3: Calcination of cathode precursor material.

Other batteries using the non-carbon coated active cathode material were also created, as a control and for comparison. This was done using the same procedure, except that the cathode precursor was never mixed with graphene. The dry gel powder material was pressed with the crimping machine by itself, after which it was calcinated in the furnace using the same times and heat rates.

3.3 Synthesis of Graphene

Using a 500 mL, three-neck flask, graphene oxide was dispersed in dimethylformamide (DMF) in a ratio of 200 mL DMF to 0.1605 g graphene oxide, as

shown in Figure 3-4. DMF acted to dissolve organics into the solution. This solution was then sonicated for one hour to ensure all of the graphene oxide was fully dissolved. While the solution was being sonicated, the reflux system was set up in the fume hood. 150 mL of hydrazine was then added to the graphene oxide solution. The hydrazine acted to reduce the graphene oxide to graphene. Once the hydrazine was added, the reflux system was purged with nitrogen for approximately 10 minutes. Once the system was purged, the nitrogen was reduced to a low-flow rate and the solution was heated to 100°C while being stirred overnight. As this was occurring, a low-flow rate of cooling water passed around the system in order to condense vapors back into the solution. The following day, the solution was allowed to cool.

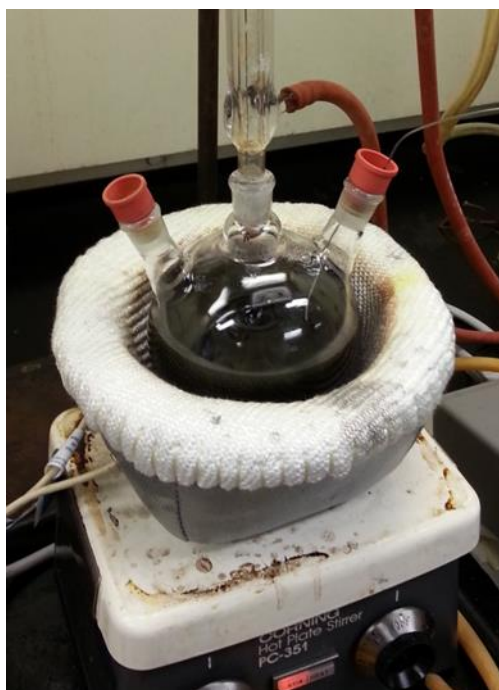


Figure 3-4: A three-neck flask with graphene oxide solution.

During the cool down period, the filtration system was set up by attaching a funnel and flask to the sink faucet, which created a pressure difference around the filter. By running tap water through the faucet, a vacuum was created in the flask allowing the solution to be pulled through the filter. The filter paper was first washed with de-ionized (DI) water. The cooled solution was then dispensed into the funnel containing the filter.

After the graphene was filtered out of the solution, the graphene was rinsed with DI water 4 times, and sequentially rinsed with ethanol 3 times. After the graphene was rinsed, the filter paper containing the graphene deposits was removed from the funnel and placed into a petri dish, as shown in Figure 3-5.

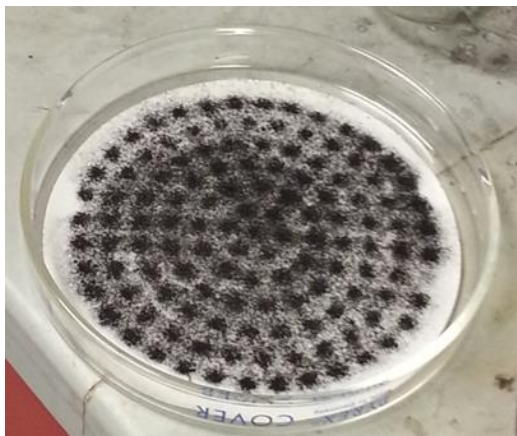


Figure 3-5: Graphene deposits in filter.

This dish was then placed into a furnace at 60°C and heated for four days to allow the graphene to completely dry. Once dry, the filter was removed from the furnace and the graphene was scraped off of the filter using a clean scalpel. The graphene was then placed into a glass vial to be stored while awaiting the next step in the synthesis process.

3.4 Slurry Coating Process

First, it was necessary to grind the active cathode material with carbon black (Alfa Aesar, 99%+) using a mortar and pestle. After the two were well ground, a poly(vinylidene fluoride) (Alfa Aesar)/N-methyl-2-pyrrolidone (NMP) (Sigma-Aldrich, 99.5%) solution was added to the mixture to create a gel-like solution. The cathode active material, carbon black, and poly(vinylidene fluoride) (PVDF) were combined in an 80:10:10 mass ratio, respectively. The PVDF solution comprised of 0.025 g PVDF/1 mL NMP. The powders and solution were ground with a mortar and pestle for approximately 30 minutes, until the slurry had a consistent texture. A section of glass was then cleaned with acetone after which a piece of aluminum foil was cut and placed

onto the glass. The surface of the foil was then cleaned with acetone and wiped dry before being taped to the glass. Using tapes of different thickness allowed control over the thickness of the slurry deposited on the aluminum foil. The slurry was poured onto the foil and smoothed out across the foil by using a glass rod, as seen in Figure 3-6.



Figure 3-6: Aluminum foil coated with active cathode material.

Once there was a uniform coating on the foil, the slurry was put in a fume hood to dry for a few days. After drying, the foil was then stamped out into battery-sized circles and placed in a covered petri dish. The dish was then moved to a vacuum furnace and heated to 100°C overnight to completely dry out the active cathode material.

3.5 Coin Cell Assembly and Electrochemical Testing

Once the cathode material was attached to a conducting sheet, a full battery could be assembled for testing. In combination with the created cathode, a pure lithium (Alfa Aesar, 99.9%) anode was used, along with a lithium hexafluorophosphate electrolyte (Syerm Chemicals, INC, 99.9%+) and a commercial grade polypropylene separator (Celgard® 2500). These were combined inside a (CR2032) coin cell shell, such as the one schematically shown in Figure 3-7. The battery was mechanically assembled within a vacuum hood containing an inert atmosphere of argon. The battery was then crimped with 1000 psi for about 15 seconds.

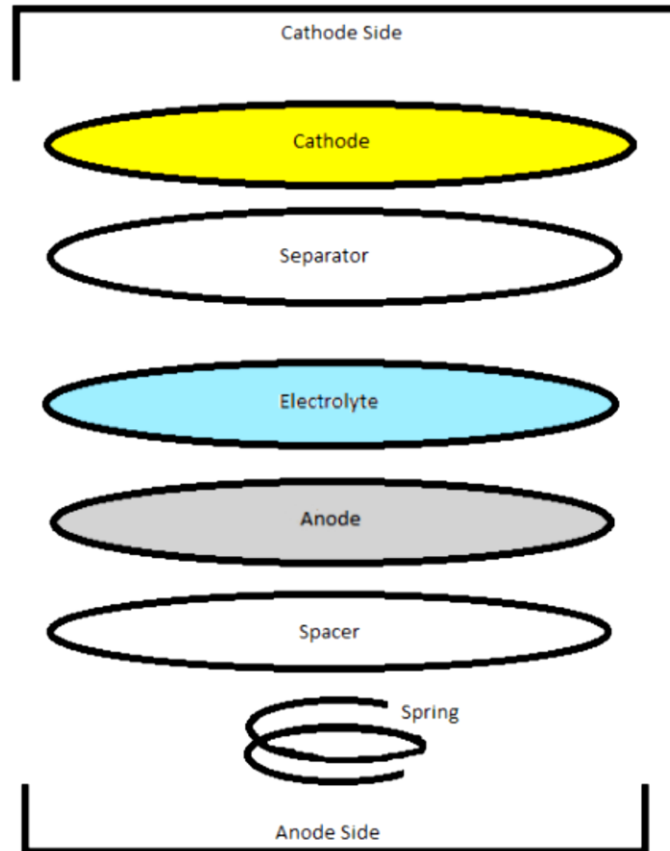


Figure 3-7: Diagram of coin-cell composition.

Once the coin-cell batteries are assembled, the electrochemical properties are tested using a MTI-EQ-BST8-10MA battery test station. The properties that were tested were the initial capacity and cycling life performance of the cell. These were tested for at a discharge/recharge rate of 0.1C for 30 cycles.

4 Results and Discussion

In this chapter, the results from the $\text{Li}_2\text{Fe}_{0.5}\text{Mn}_{0.5}\text{SiO}_4$ cathode synthesis and electrochemical testing are presented and discussed.

4.1 Cathode Synthesis

A major aspect of our research was synthesizing the cathode, consisting of $\text{Li}_2\text{Fe}_{0.5}\text{Mn}_{0.5}\text{SiO}_4$ and graphene. It was important to characterize the cathode materials using SEM in order to determine the average particle size and the distribution of particle size. It was also important to conduct XRD analysis to determine the phases present in the final cathode.

4.1.1 SEM Analysis

Figures 4-1 and 4-2 show SEM images for pure $\text{Li}_2\text{Fe}_{0.5}\text{Mn}_{0.5}\text{SiO}_4$ baked at 700 degrees C for 10 hours and 14 hours, respectively. The image in Figure 4-1 is magnified 10,000 times, while the image in Figure 4-2 is magnified 5,000 times. The sample that was baked for 10 hours showed a smaller particle size of around 350 nanometers, with a very well-distributed particle size throughout the sample. The sample that was baked for 14 hours had a larger particle size of between 2 micrometers and 0.1 micrometers, a larger distribution of particle size throughout the sample. Both samples demonstrate a spherical morphology.

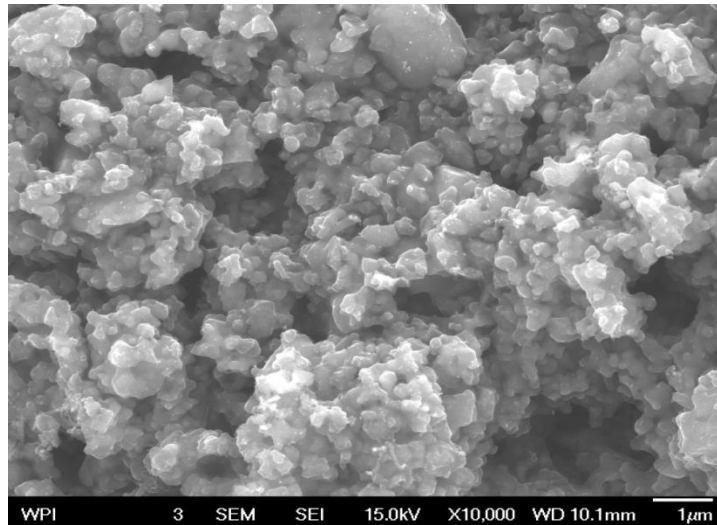


Figure 4-1: An SEM image for pure $\text{Li}_2\text{Fe}_{0.5}\text{Mn}_{0.5}\text{SiO}_4$ baked at 700°C for 10 hours.

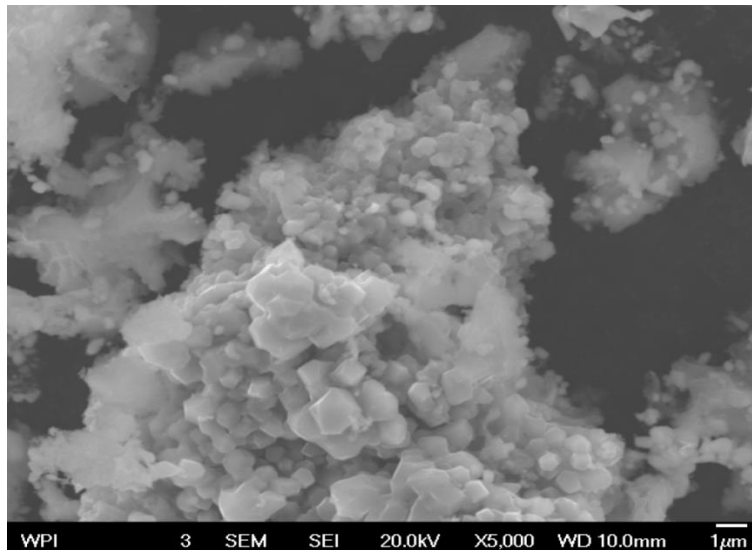


Figure 4-2: An SEM image for pure $\text{Li}_2\text{Fe}_{0.5}\text{Mn}_{0.5}\text{SiO}_4$ baked at 700°C for 14 hours.

Increased surface area within the cathode theoretically increases the charge capacity of the battery. The smaller particle size obtained through baking the pure lithium compound for 10 hours is the most desirable, as the small particle size increases the surface area within the cathode. The SEM image shown in Figure 4-3 shows the successfully synthesized graphene nanosheets with small sizes, as well.

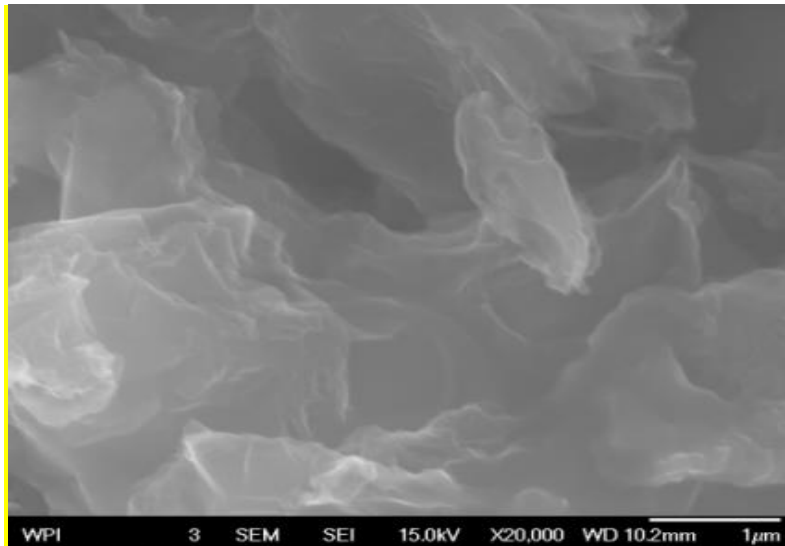


Figure 4-3: An SEM image of graphene nanosheet.

4.1.2 XRD Analysis

Integral to the project is providing proof of the presence of the recorded materials used in the proper proportions. Through XRD analysis, we sought to do just that, but instead encountered the recurring presence of one pure iron, in addition to the materials we were supposed to synthesize. One may observe in Figure 4-4 the high peak in the center being identified as part of a series of peaks, showing pure iron to be in the mix. One may find additional data showing the presence and evidence of the pure iron present in the sample with the JADE data in Appendix 6.1. We are unsure of the cause of this peak.

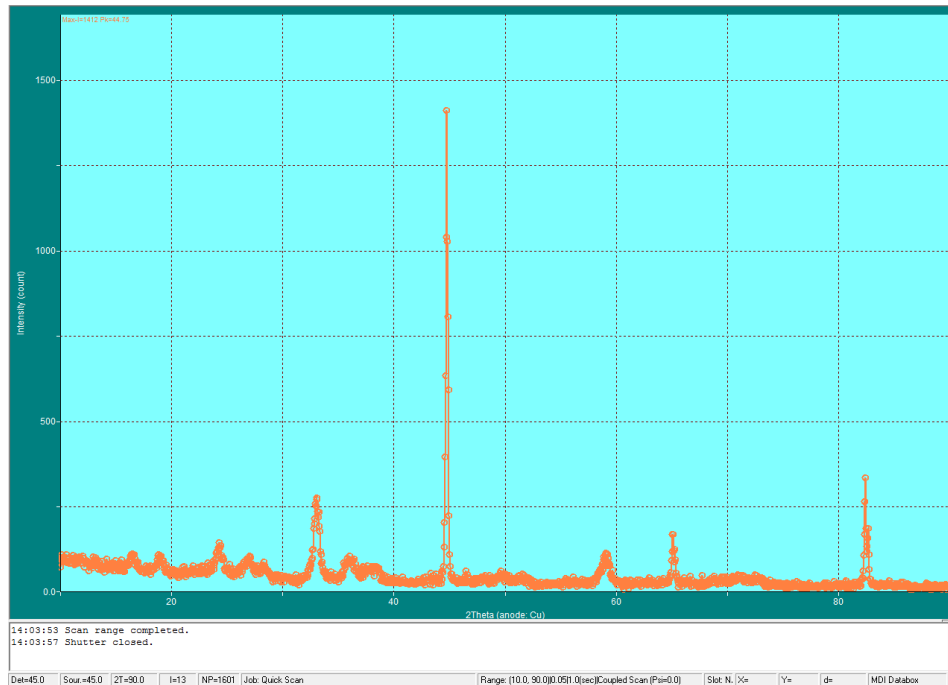


Figure 4-4: XRD data showing a pure iron peak.

While the XRD data showed a pure iron presence, the data found with the energy dispersive x-ray spectroscopy (EDX) feature of the SEM shown in Figure 4-5, one may see the presence of the proper materials of our lithium silicate. Additional EDX data on the composition of our cathode material can be found in Appendix 6.2.

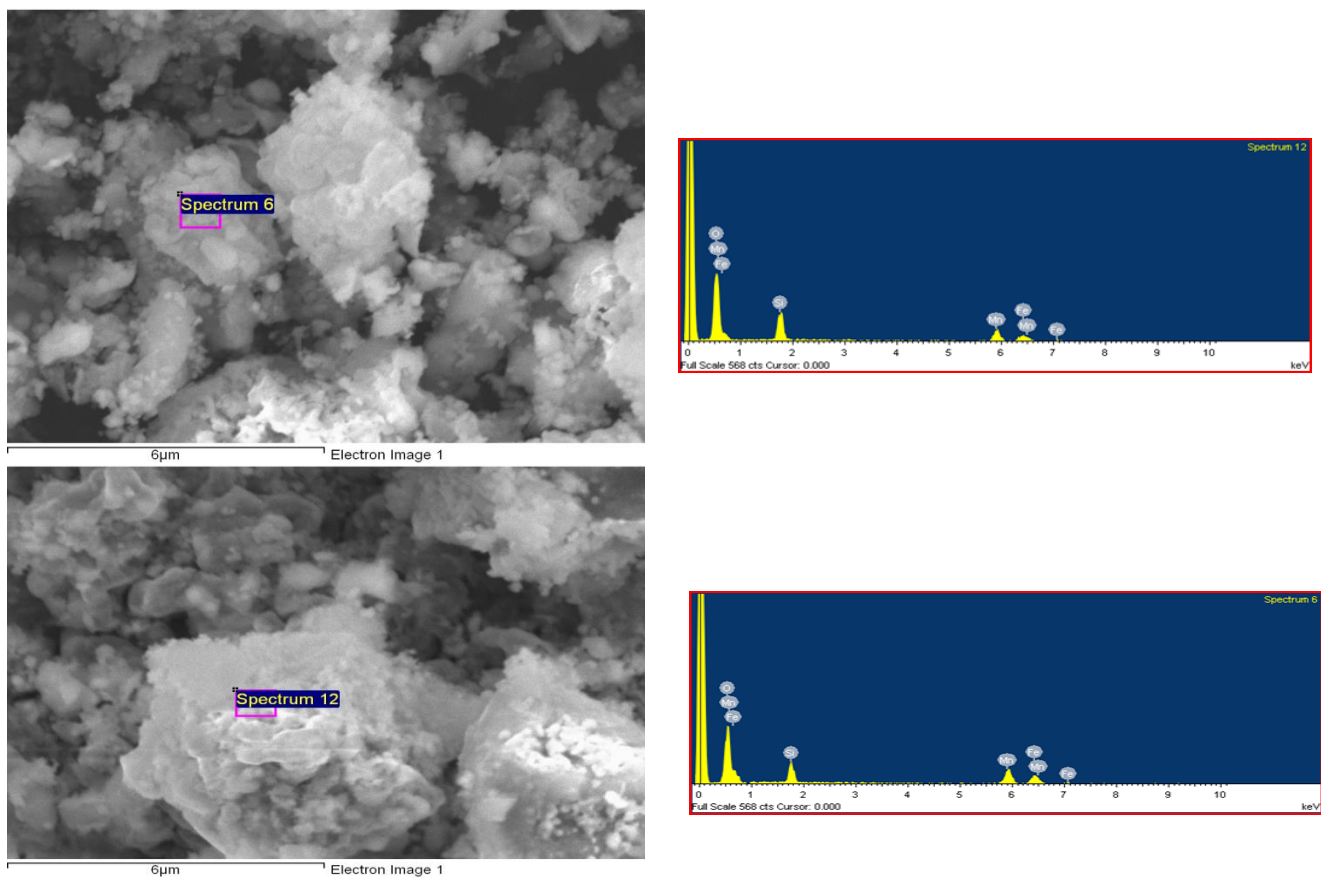


Figure 4-5: EDX images for pure $\text{Li}_2\text{Fe}_{0.5}\text{Mn}_{0.5}\text{SiO}_4$ – 700°C for 10 hours.

4.2 Electrochemical Testing

This portion of the project was to show the effects of the graphene coating on the batteries' performance. From the graph in Figure 4-6 below, one may observe a higher and relatively stable discharge capacity at approximately 54 mAh/g for the graphene coated sample, as compared with the low capacity at approximately 15 mAh/g for the non-coated samples.

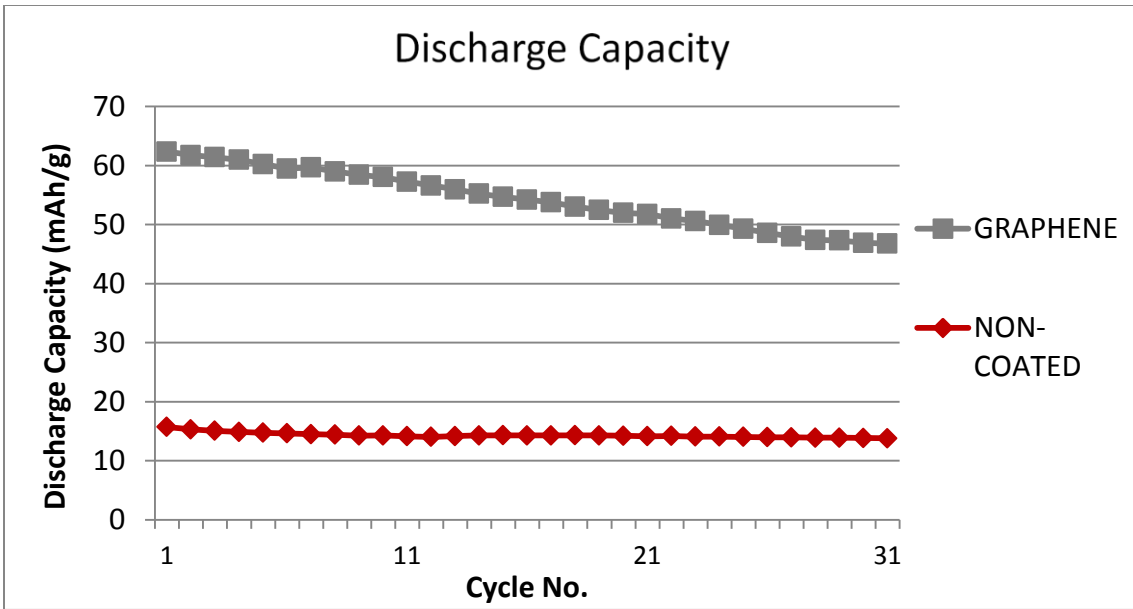


Figure 4-6: Comparative test data between discharge capacities of coated and uncoated silicates.

Additionally, the graphene coated battery samples had a current efficiency that sustained with increasing cycles, averaging around 97 percent as seen in Figure 4-7 below. While the non-coated samples eventually reached a similar current efficiency, the efficiency took ten cycles to reach, thus showing a lesser ability to carry a charge.

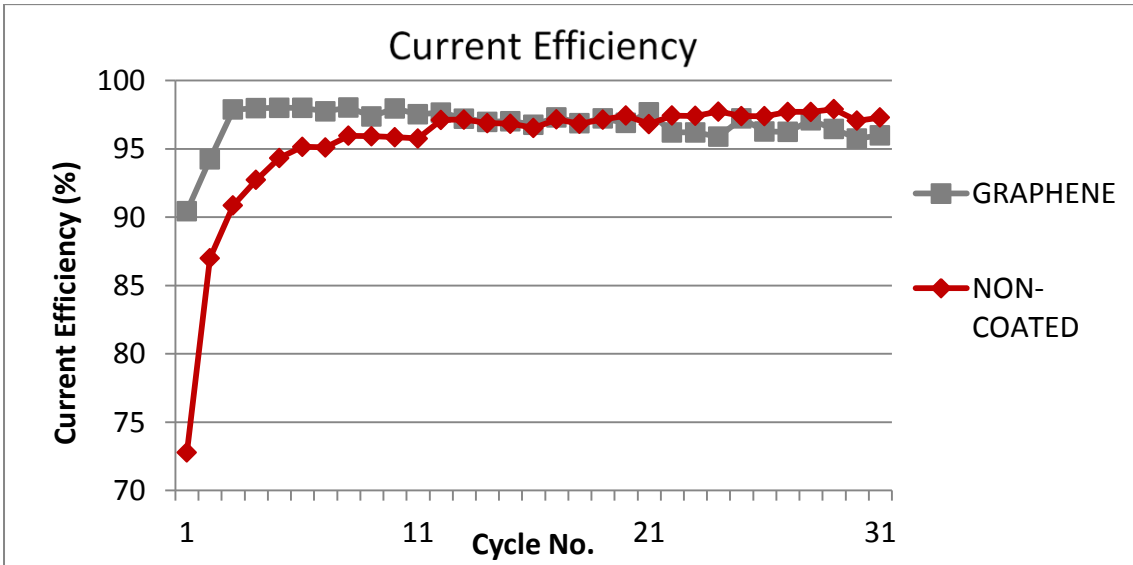


Figure 4-7: Comparative test data between current efficiencies of coated and uncoated silicates.

4.3 Results Discussion

With the conclusion of our project, we have found some success and some unexplained phenomena. Through SEM analysis, we observed the outcome of the lithium silicate synthesis producing a sample of similarly sized particles with a desirably small average 350 nm diameter, though differing with the time spent heating in the furnace. Although we followed the tried and true methods for both the lithium silicate and graphene syntheses, we found that the materials did not perform as well as known counterparts seen in Appendix 6.3 in discharge capacity, but maintained a comparable current efficiency. The poor comparative capacity to both the previously tested graphene coated samples and sucrose coated samples would indicate that there was something amiss with the lithium silicate material, but the graphene synthesized was still good.

5 Conclusions and Recommendations

The results of our work show that the graphene coating improves the battery performance and overall consistency as compared with cathodes coated in carbon extracted from sucrose, and non-coated lithium silicate cathodes. The graphene coated lithium silicate cathodes demonstrated high initial and continued current efficiency of the batteries, improved cycle life, and high capacity compared with the non-coated cathodes. This demonstrates that graphene coated $\text{Li}_2\text{Fe}_{0.5}\text{Mn}_{0.5}\text{SiO}_4$ cathode materials are a promising advance in energy storage.

Going forward, we recommend reviewing the reviewing present processes and optimizing the know methods. We recommend reviewing the XRD process to determine the cause of noise within the resulting data sets. We also recommend evaluating the synthesis process to see where contamination may have been introduced to result in incomplete cathode synthesis, and to decrease or eliminate human errors within the process. The next step with this project would be determining the optimal length of time for the calcination reaction to result in small, evenly-sized particles while still allowing for a complete reaction. Particle size can also be optimized by utilizing a more effective mechanical processing method to crush the cathode, such as use of a ball-milling machine rather than use of a mortar and pestle. We believe that continued research on lithium silicates is both necessary and viable for the future of electronics.

6 Appendices

6.1 Comparative XRD Data Findings

This appendix contains additional XRD images and findings from the cathode samples.

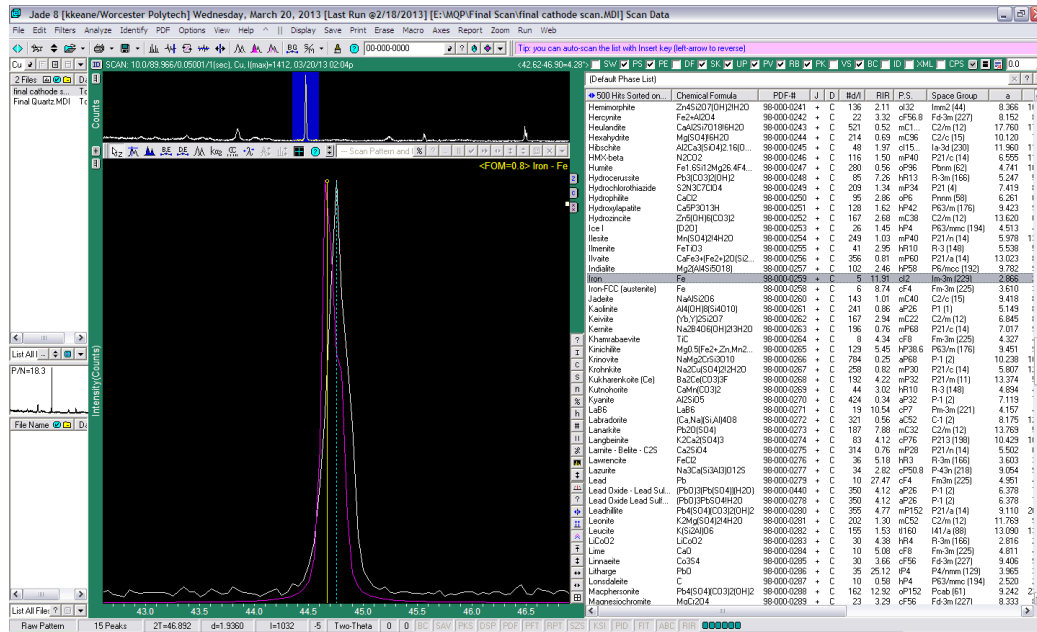


Figure 6-1: The full range of 2theta for the pure iron comparison.

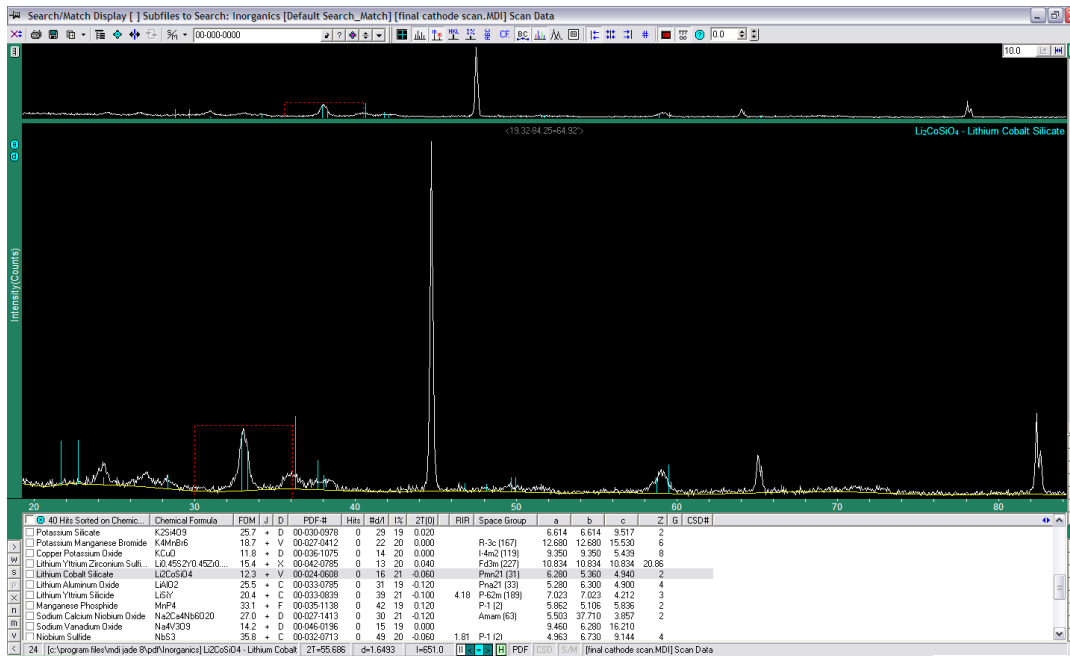


Figure 6-2: Full comparison to lithium cobalt silicate data.

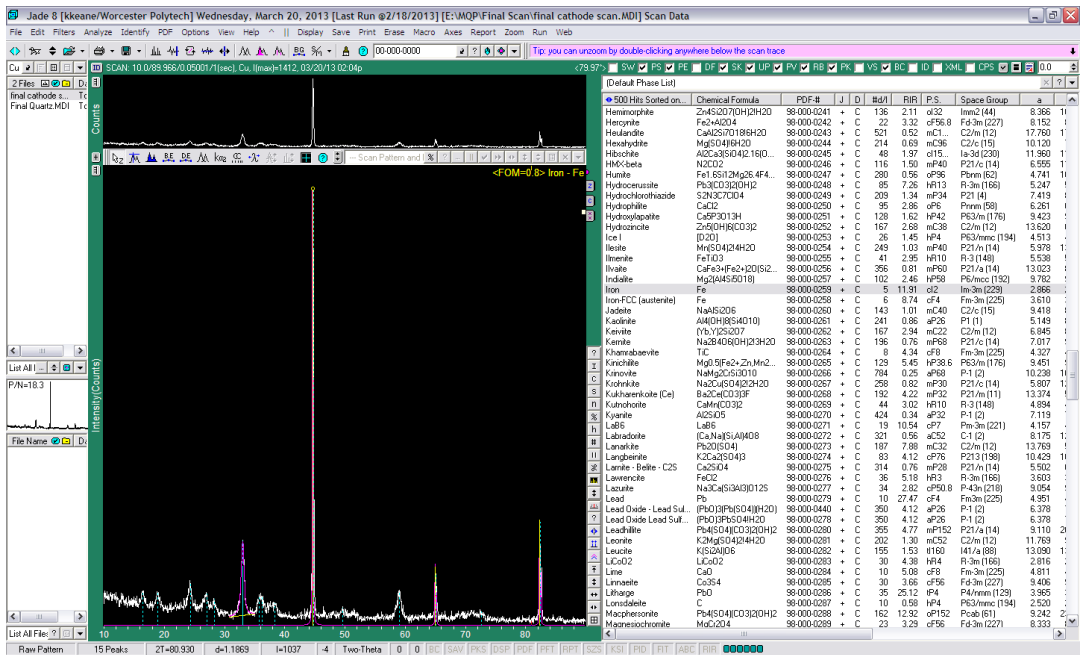


Figure 6-3: Full comparison to lithium cobalt silicate data.

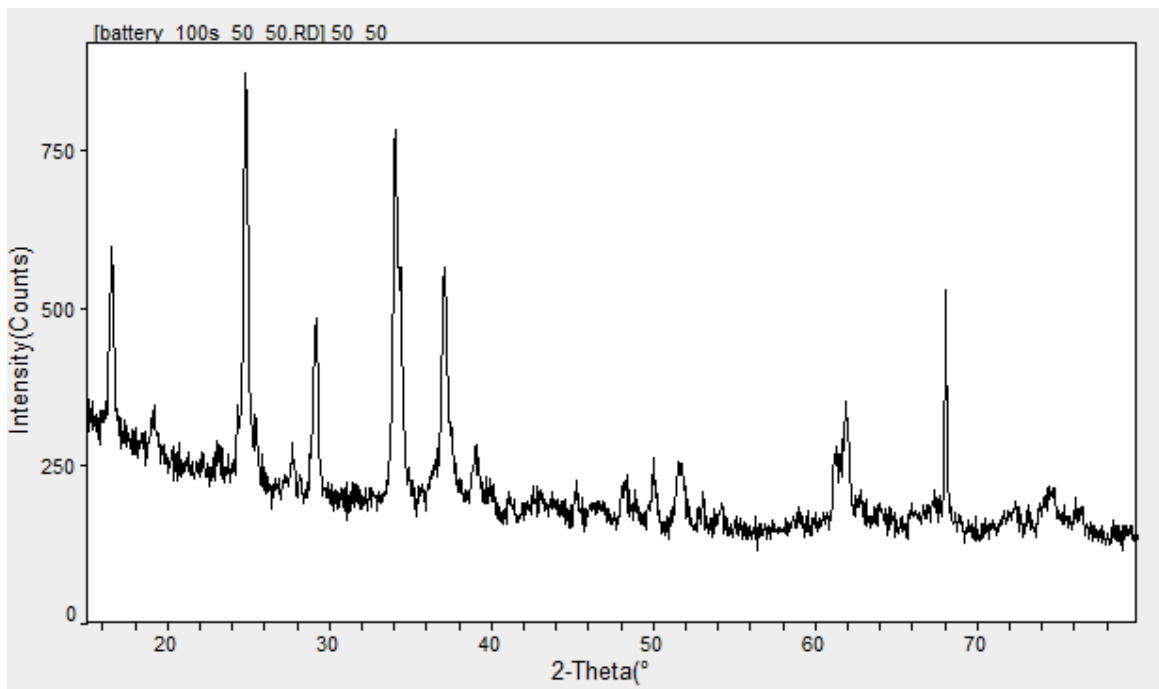


Figure 6-4: 2theta comparison to previous XRD data of carbon-coated cathode material without singular, large peak.

6.2 EDX Data

Below is the complete data set from an EDX scan on the seventh spectrum of our non-coated cathode material.

Project 1

Spectrum processing:

No peaks omitted

Processing option: All elements analyzed (Normalised)

Number of iterations = 2

Standard:

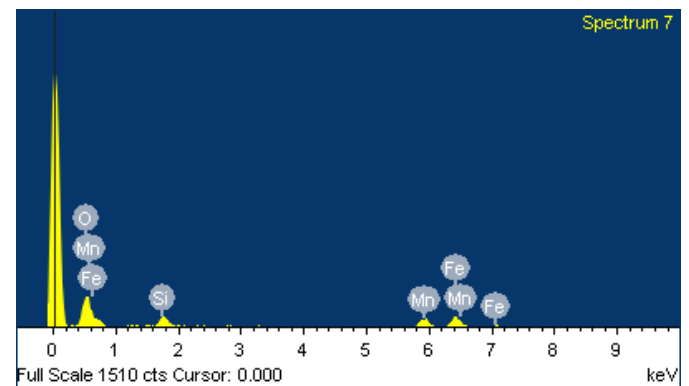
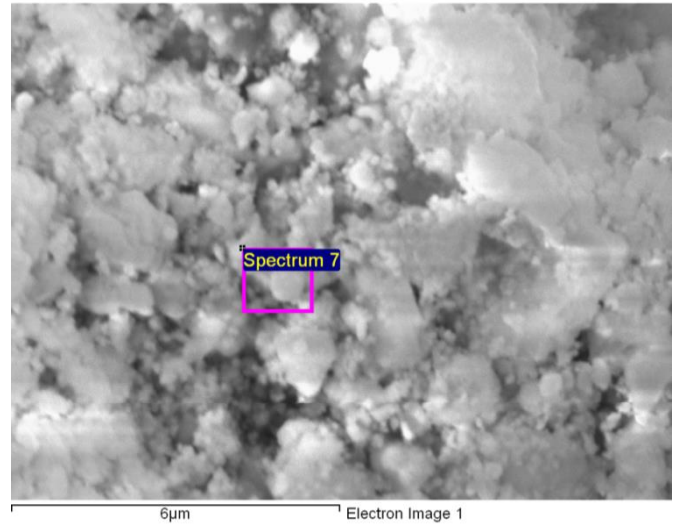
O SiO₂ 1-Jun-1999 12:00 AM

Si SiO₂ 1-Jun-1999 12:00 AM

Mn Mn 1-Jun-1999 12:00 AM

Fe Fe 1-Jun-1999 12:00 AM

Element	Weight%	Atomic%
O K	35.67	63.39
Si K	7.29	7.38
Mn K	23.73	12.28
Fe K	33.31	16.96
Totals	100.00	



Comment:



6.3 Comparative Electrochemical Test Data

The figures below show the electrochemical test data for the graphene coated lithium silicate samples made and tested by WPI graduate student researcher Yinjie Cen with black markings, the sucrose coated samples of the WPI 2012 MQP research team referred to earlier with the grey markings, and our own graphene coated samples with the red markings. The data clearly shows the underperformance of the discharge capacity for our samples, but comparative current efficiency performance.

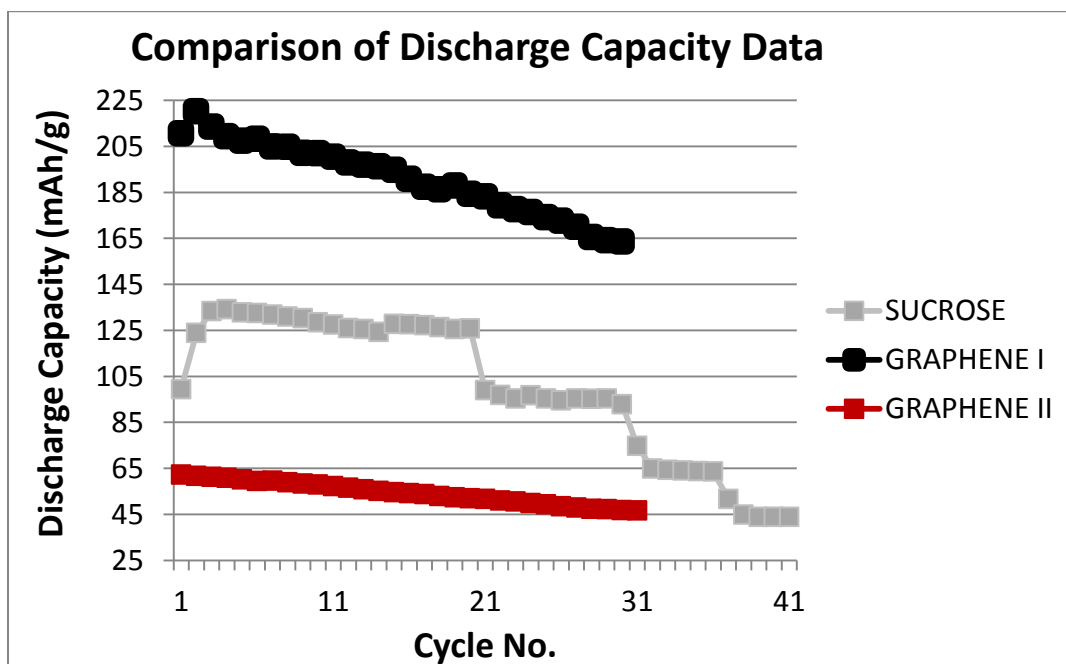


Figure 6-5: Comparisons of coatings on the discharge capacities from different research projects.

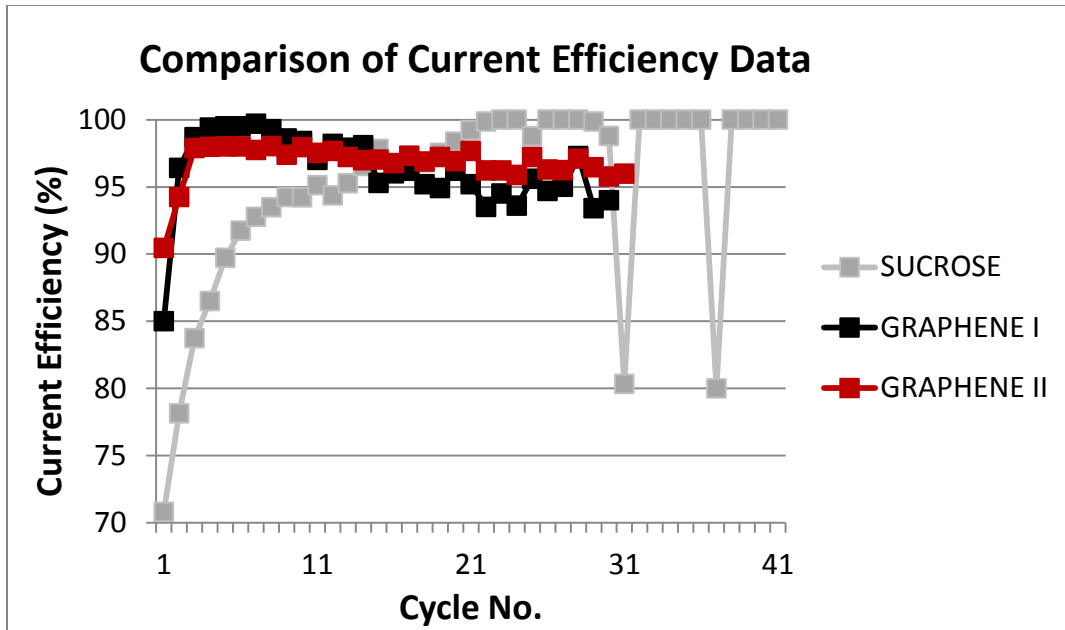


Figure 6-6: Comparisons of coatings on the current efficiencies from different research projects.